NASA Technical Paper 3234

September 1992

Applications of a Direct/Iterative Design Method to Complex Transonic Configurations

Leigh Ann Smith
and Richard L. Campbell

NASA

NASA Technical Paper 3234

1992

Applications of a Direct/Iterative Design Method to Complex Transonic Configurations

Leigh Ann Smith
and Richard L. Campbell
Langley Research Center
Hampton, Virginia

National Aeronautics and Space Administration
Office of Management
Scientific and Technical Information Program

Abstract

The current study explores the use of an automated direct/iterative design method for the reduction of drag for transport configurations, including configurations with engine nacelles. The method requires the user to choose a proper target-pressure distribution and then develops a corresponding airfoil section. The method can be applied to two-dimensional airfoil sections or to three-dimensional wings. The three cases that are presented show successful application of the method for reducing drag from various sources. The first two cases demonstrate the use of the method to reduce induced drag by designing to an elliptic span-load distribution and to reduce wave drag by decreasing the shock strength for a given lift. In the second case, a body-mounted nacelle is added and the method is successfully used to eliminate increases in wing drag associated with the nacelle addition by designing to an arbitrary pressure distribution that has an elliptic span-load distribution with reduced shock strength. The third case does not show a large drag decrease, but does demonstrate the elimination of nacelle influence on the original pressure distribution as a result of the redesigning of a wing in combination with a given underwing nacelle to clean-wing, target-pressure distributions. These cases illustrate several possible uses of the method for reducing different types of drag. The magnitude of the obtainable drag reduction varies with the constraints of the problem and the configuration to be modified.

Introduction

Drag reduction is an important consideration in any aircraft design. While drag can never be eliminated, its minimization will result in reductions in fuel consumption for transport aircraft. Drag reduction can also extend the range or reduce the time to destination for both commercial and military vehicles. When drag is reduced, the engine power needed to overcome it is reduced; therefore, smaller and quieter engines can be used. Smaller engines mean less weight and a further reduction in drag.

Historically, reducing the drag of a given vehicle has meant many hours of wind-tunnel testing, involving modifications to the configuration through a cut-and-try approach. With the advent of computational fluid dynamics (CFD), the cut-and-try approach has been updated to take advantage of analytical techniques. Currently, one of the more promising methods of drag reduction is automated design. A considerable amount of development work has been done in this area. There is a wide spectrum of unique design codes available. These codes can also be used for functions besides drag reduction, such as controlling pitching moment. While design methods exist for a variety of aircraft components and flow conditions, this paper focuses on drag reduction in transonic wing design, including design in the presence of nacelles.

Automated design methods can be used to reduce specific types of drag, such as wave drag, viscous drag, induced drag, and interference drag. The following discussion identifies four major classifications of design methods and addresses their advantages and disadvantages in the area of drag reduction. These categories are optimization methods, fictitious gas methods, inverse methods, and direct/iterative methods. The first two types of methods can be used to address drag directly, while the second two types address drag through the modification of a pressure distribution. One disadvantage common to all these methods is that they typically produce single-point designs, which have favorable characteristics at the design flow conditions but unknown performance under other conditions.

Optimization methods (Hicks, Murman, and Vanderplaats 1974; Kennelly 1983) directly address the reduction of drag for an airfoil or wing. These methods identify drag as an objective function and then systematically perturb the design until the drag function reaches a minimum. The drag function that is minimized can be total drag or some specific drag component. Optimization methods can be constrained to allow certain characteristics to be maintained while performing a design. Two disadvantages of these methods are that they can require an order of magnitude more computer time for their search

than other types of methods as discussed by Slooff (Anon. 1990) and can sometimes only reach a local minimum.

Fictitious gas methods have been developed to directly eliminate wave drag (Sobieczky et al. 1979). By using these methods, the designer can eliminate shocks from the flow around an airfoil. This method is called fictitious gas because the density of the gas in the supersonic region is altered to allow the potential-flow equations to remain elliptic. The supersonic region is then recomputed from the potentials on the sonic surface. A new streamline that intersects the old surface is used as the new airfoil shape. By definition, these methods cannot generate designs with shocks, which are often unavoidable and sometimes desirable (if weak) at transonic conditions as discussed by Whitcomb (Anon. 1980).

Inverse methods (Volpe and Melnik 1985; Giles and Drela 1986) and direct/iterative methods (Campbell and Smith 1987) are two separate classes of methods, but they appear similar to the user. Neither method can address drag directly, but both can reduce drag with a low-drag target-pressure distribution. Both methods iteratively modify a starting geometry until the target-pressure distribution is reached. The techniques for modifying the airfoil shape distinguish the two types of methods. Direct/iterative methods directly solve the flow about a given geometry and use an algorithm to modify airfoils based on the difference between the current and target pressures. This process is iterated until the differences become small. Inverse methods solve the flow in reverse by using specified local flow velocities as boundary conditions and solving for the geometry that meets the flow tangency requirements. Boundary-layer thickness can be accounted for by subtracting it from the final design shape. Typically a direct/iterative method is easier to develop, because its algorithm can be installed in any existing flow solver.

All methods that require a target-pressure distribution can address specific types of drag by the design of that distribution. For example, reducing the slope of an adverse pressure gradient can delay separation and reduce viscous drag. A disadvantage of working with target pressures is that, while the surface pressures may be free of shocks as specified, a strong shock may develop in the flow field just above the designed surface (Volpe 1990). Also, constraints are needed to ensure that the designs produced are physically possible (e.g., no crossed trailing edges).

Poor correlation between calculated drag values and experimentally determined values is a key issue when discussing design for reduced drag. To be reliable, any calculated improvements in the drag coefficient of a configuration should be larger than the error band for that particular method of drag computation as discussed by Henne (Anon. 1990).

The current study explores the use of the Direct/Iterative Surface Curvature (DISC) design method for the reduction of drag for transport configurations. Since the method is a direct/iterative method, specific types of drag can be reduced by modifying pressure distributions. The various examples shown demonstrate a reduction of induced drag by using elliptical span loading, a reduction of wave drag by modifying target-pressure distributions for decreased shock strength, and a reduction of the interference drag associated with nacelles by recontouring the wing in the presence of the nacelle.

Symbols

AR	aspect ratio
C_L	wing-body lift coefficient
C_p	pressure coefficient
c	local chord
c_{ave}	average chord
c_l	section lift coefficient
DISC	Direct/Iterative Surface Curvature design method
e	Oswald's efficiency factor
M	Mach number
TTE	twist-to-elliptic
WB	wing-body
WBN	wing-body-nacelle
WBPPW	Wing-Body-Pod-Pylon-Winglet code
x	streamwise coordinate
y	vertical coordinate
η	fractional spanwise location (see fig. 1)

Description of Design Method

Design Algorithm

The DISC method of Campbell and Smith is used in this study. The basis of the method is described in Campbell and Smith (1987), and applications and extensions are discussed in Smith and Campbell (1991). This automated design method computes modifications to an airfoil or wing by use of an algorithm

that relates changes in local velocity to changes in surface curvature. A target-pressure distribution is required as input. The method is coupled with a suitable aerodynamic code that is used to analyze a geometry at the design flow conditions to obtain a pressure distribution. This pressure distribution is compared with the target-pressure distribution in the design module, and the geometry is modified based on the differences. Each new geometry is analyzed in the aerodynamic code to obtain an updated set of pressures. This process is continued for a preset number of cycles. The choice of aerodynamic analysis code can allow the method to include viscous and aeroelastic effects.

As part of this study, the DISC method was extended to allow design to a target span-load distribution by modifying and smoothing the twist distribution of a wing. This algorithm is separate from the surface curvature modification, although the two can be done concurrently. The target span load is obtained as follows. Based on an analysis of the configuration, the incidence angle of each section is adjusted to drive it toward the target c_l for that section. After each section is adjusted, the twist distribution is smoothed along the span of the wing to eliminate abrupt changes in twist from one station to the next. The configuration is then reanalyzed, and new adjustments are made. This pattern of analysis, adjustment, and smoothing continues for the preset number of cycles.

Aerodynamic Analysis

For this study, the Wing-Body-Pod-Pylon-Winglet (WBPPW) transonic small-disturbance code (Boppe 1987) was used in combination with the design method. It has the capability of modeling both two-dimensional airfoils and complex three-dimensional aircraft geometries at transonic speeds and has been applied to a wide range of configurations. The code solves a version of the transonic small-disturbance equation that has been extended to yield improved results for configurations with swept shocks. Flow solutions for a wing-body case are acquired through calculations on two rectangular grid systems: a global crude grid and an embedded fine grid on the wing. Since the wing boundary conditions are applied on a plane, only the boundary conditions need to be updated after a design cycle; it is not necessary to modify the grid. A two-dimensional strip boundary-layer approximation based on the method of Bradshaw and Ferriss (1971) is used to simulate viscous effects.

Since the focus of this study is drag reduction, a brief discussion on the accuracy of the methods used to compute the drag for the test cases follows. Waggoner (1980) noted that for an advanced transport configuration with a supercritical wing, a wing-body version of the WBPPW code was not able to predict absolute drag levels very accurately, but could compute drag increments within about 5 counts of experimental values for conditions with weak shocks. Experience has indicated that this correlation deteriorates for conditions with stronger shocks, primarily because of the pressure integration approach used in the code. The drag coefficients used in this study were therefore computed by combining an estimate of the wave drag from a method based on the approach of Lock (1985) with the induced drag value calculated in the WBPPW code. Lock estimates his method has an error band of -10 percent to 30 percent of the calculation. The induced drag for the configuration is computed by the commonly used formula $\frac{C_L^2}{\pi \mathrm{AR} e}$, where Oswald's efficiency factor e is determined by means of a fast-Fourier analysis applied to the configuration span-load distribution. Since the span-load distribution is computed fairly accurately for a given configuration lift coefficient, the error band of the induced drag computation should be about ± 5 percent of the computed value.

Results and Discussion

The following test cases illustrate various applications of the design method. These cases demonstrate the use of the design method to reduce drag by designing to target pressures with low shock strengths and elliptical span loadings. Reduction of nacelle influence is demonstrated by designing to clean-wing target pressures in the presence of nacelles. Even though viscous drag reduction is not addressed in this study, local Mach numbers are held below 1.3 to reduce the chance of separation as demonstrated by Haines (1987). No attempt was made to constrain other parameters, such as pitching moment, in this study. All designs were run for 90 cycles, which allowed more than adequate convergence of the design process. Convergence was determined by inspection.

Case 1—Elliptic Clean Wing

To test the effectiveness of the design method in reducing wave and induced drag, a wing-body configuration was redesigned to an elliptic span load. This redesign was done in two parts. First, the twist distribution was changed to obtain the elliptic span loading; second, the airfoils were redesigned to reduce shock strength.

A generic executive-jet configuration with an axisymmetric body, a 23° swept wing, and an aspect

ratio of 7.1 was used as the baseline. The planform is shown in figure 1. The values of η shown in figure 1 represent the locations of design changes. These changes were then linearly interpolated for the area between stations. An overwing nacelle is shown in this figure, but nacelle effects are not considered until case 2. All analyses conducted on the executive-jet configuration were performed at $M = 0.79$ and $C_L = 0.55$.

An analysis of the baseline configuration showed that this shape had an efficiency factor e for the wing of 0.986 and an induced drag coefficient of 0.0140. To bring the baseline to an elliptic span loading, and to modify the twist distribution of the wing, the new twist adjustment extension (twist-to-elliptic, TTE) was activated. Figure 2 illustrates the change. The twist values along the wing were adjusted by as little as 0.2° inboard to as much as 1.9° near the mid semispan. Twisting the wing to achieve this elliptic load distribution increased the value of e to 0.994, decreased the computed induced drag coefficient by 0.0004, and increased the wave drag by 0.0002 from the baseline values. These numbers show the trends associated with twisting the wing but are not large enough to be significant when computational accuracy is considered.

To further decrease drag, shock strengths were weakened for the elliptically loaded wing by redesigning the wing pressure distributions at each station. An analysis of the elliptically loaded wing was performed to establish the corresponding wing pressures. These pressure distributions were modified to reduce shock strength and were then used as target pressures for a new design. The design philosophy was to lower the local Mach number ahead of the shock (i.e., increase the pressure), thus reducing the shock strength and associated wave drag. A possible additional benefit of this philosophy is to delay or remove separation (Haines 1987). When modifying the pressure distributions, the section lift coefficients were retained so that the elliptic span-load distribution was maintained. No other considerations, such as pitching moment, were addressed. These target-pressure distributions simply represent possible designs developed by the authors and in no way represent the "optimum" distributions.

Figure 3 shows a typical target-pressure distribution and design history. Comparison of the initial and final curves illustrates the magnitude of the changes made in these design exercises. Comparison of the final and target curves illustrates the accuracy with which target-pressure distributions are achieved. Thus, analysis pressures of DISC designs shown in figure 4 do not differ substantially from the target pressures used to produce the designs.

Figure 4 shows the pressures associated with the analysis of the baseline configuration, the elliptically loaded wing (TTE), and the wing redesigned using the DISC method. The pressures are shown at 3 stations along the wing. At each station, use of the DISC method resulted in some reduction in shock strength. Figure 5 shows the differences between the baseline and redesigned airfoils. The vertical scale is expanded to show detail. The root and mid semispan show only minimal changes in airfoil thickness and contour, while the outboard station shows a decrease in thickness of 1.4 percent chord.

Table 1 shows the drag coefficients obtained in each step of the design process. The change to elliptic span loading (TTE) produced only a slight decrease in induced drag, because the original configuration was nearly elliptic. This change also increased the wave drag. The target-pressure recontouring (DISC) produced a substantial reduction in wave drag, and the total drag coefficient was decreased by 0.0033 from the baseline.

Case 2—Elliptic Wing With Nacelle

After the clean-wing design was developed, the overwing, body-mounted nacelle (fig. 1) was added to the configuration. This arrangement is typical of current business jets and can profoundly affect the flow over the wing root area. To determine this effect, the new configuration was analyzed by using WBPPW. The addition of the nacelle caused a sharp drop in inboard lift and a loss of the elliptic span loading. (See fig. 6.) To regain the elliptic span loading, a design was carried out that used the clean-wing pressures developed in the previous case as targets and the DISC geometry designed in case 1 with the nacelle added as the starting shape. This effort was moderately successful. Outboard, the target pressures were attained with only minimal changes to the airfoil sections. Inboard, however, where the nacelle has the most effect, the target pressures were only met over a portion of the surface (fig. 7), and the airfoil sections became extremely thick (20 to 25 percent).

To compensate for the effects of the nacelle, the clean-wing pressures were modified to obtain new target pressures. Although changing the position or contours of the nacelle could relieve its influence on the flow, it was assumed in the context of this sample case that the nacelle position was fixed and that only the wing contours could be modified. Several steps were taken to revise the target pressures. The

distributions were shifted to slightly more positive pressures to reduce airfoil thickness. Shock strengths were reduced at some stations. Also, some aft loading was added to maintain the required section lift coefficient, but no consideration was given to pitching moment. The revised target pressures were then used to compute a new wing shape, again starting from the geometry developed in case 1 with the nacelle added.

Shown in figure 8 are pressures from an analysis of the clean-wing design (nacelle off) of case 1 and an analysis of the nacelle-on design. This figure illustrates the differences in pressures necessary to compensate for the nacelle. Airfoil sections of the nacelle-on wing design are compared in figure 9 with the nacelle-off (clean wing) design of case 1. The root airfoil shows some twist and increased thickness relative to the nacelle-off design. The mid semispan station airfoil is considerably thinner than the nacelle-off airfoil and might require additional design work to be practical. At the tip, the nacelle-on airfoil shows some rotation and slightly more aft camber than the nacelle-off airfoil.

A span load obtained from analysis of the design is shown in figure 10. The figure shows that elliptic loading has been approximated for the nacelle-on case. Table 2 compares drag coefficients for the generic, nacelle-on executive-jet configuration with the nacelle-on DISC design. Substantial improvements are again seen in drag. For this case, the wave drag coefficient is reduced by 0.0123 and the induced drag coefficient by 0.0018. Both these increments are considerably larger than the error bands on the respective drag computations. A comparison of tables 1 and 2 shows that, because of the refinements made to the target-pressure distributions, the nacelle-on design has lower drag measurements than the clean-wing design. One of the results of this refinement was a decrease in wing thickness at the mid semispan, which typically yields reduced drag.

Case 3—High-Wing Transport

The third case demonstrates the use of the method for a slightly different type of nacelle integration problem. The goal is to maintain the clean-wing pressure distributions for this case while adding underwing nacelles. This combination is possible because underwing nacelles do not perturb the flow as greatly as the inboard overwing nacelles that were used in the previous case. A transport-type configuration with a high wing is used (Lee and Pendergraft 1985). The wing has an aspect ratio of 7.52 and a quarter-chord sweep of 30°. Figure 11 shows the planform of the configuration, the nacelle location, and the stations where the design work was performed. Only a small portion of the nacelle was directly under the wing; the rear of the nacelle was at about 40 percent chord for the inboard station and about 25 percent chord for the outboard station.

Computations that are detailed in this section were performed at a Mach number of 0.807 and an angle of attack of 2.25° and resulted in a lift coefficient of 0.60. These conditions were used in an attempt to match experimental pressure distributions obtained by Lee and Pendergraft near the cruise condition.

To test the ability of the design method to remove the nacelle effect, the magnitudes of pressure changes due to the presence of the nacelle needed to be similar computationally and experimentally. A reasonably good match between experiment and computation was made for the clean-wing configuration (fig. 12), but discrepancies were noted for the full configuration. The computations did not show the effect of the nacelle installation on the upper surface pressures, and the effect, while present, was smaller on the lower surface. Similar discrepancies were shown by Waggoner of Vought Corporation in 1982 and were attributed to insufficiencies in the way the WBPPW code models the pylon geometry. The code allows only for a pylon directly under the wing, and the actual pylon extended substantially ahead of the wing.

To compensate for the inadequacies in the nacelle-on prediction, the nacelle geometry was altered slightly by using the following approach. The differences between wind-tunnel and analysis pressures were computed for the lower surface of the wing adjacent to the nacelle. An adaptation of the design algorithm was then used to change the nacelle curvature at several stations to correspond to the required changes in wing pressure for the wing station just inboard of the nacelle ($\eta = 0.33$). The nacelle curvatures were altered only on the rear portion of the nacelle, under the wing, where there is a direct relationship between surface contour and pressures. The results of the modifications are shown in figure 13. The upper surface pressures were not affected by this change, and the separation on the lower surface (fig. 13(b)) was not reflected in the result; the boundary-layer calculation in the WBPPW code is not adequate to predict the behavior of separated flows. However, this modification improved the agreement between experimental and computational pressures on the forward portion of the lower wing surface and increased the magnitude of the nacelle influence in that area. Therefore, this altered nacelle was used in all the results discussed in the remainder of this section.

The design process was then initiated to remove the nacelle effects that were predicted by the code. The design process used analytically obtained clean-wing pressures as targets and the nacelle-on configuration as the starting geometry. The resulting wing-body-nacelle configuration yields the same wing pressures as the original wing-body configuration. Figure 14 presents pressures from a nacelle-off analysis of the original configuration (WB), a nacelle-on analysis of the original configuration (WBN), and an analysis of the new configuration with the redesigned wing and nacelles on (DISC WBN). Figure 14 illustrates the significant effect of the presence of the nacelles on the lower surface pressures; this effect was eliminated by recontouring with the DISC method. Figure 15 presents the changes in airfoil shape. The new airfoils show a change in incidence angle and an increase in thickness, primarily in the midchord region.

Table 3 details drag comparisons for the original and the redesigned nacelle-on configurations. Because the span load was similar for the two wings, the induced drag remained the same. The wave drag decreased by 0.0003. This decrease is small, as was expected, because the changes in pressure occur primarily on the lower surface, where no shock is present. More sophisticated drag measurement techniques need to be applied to fully evaluate the drag reduction for this particular case.

Further computations were made to investigate the performance of the new wing shape at an off-design condition. First, the baseline wing-body configuration with the original nacelle and with the modified nacelle was analyzed at a Mach number of 0.7. These results are compared with experimental data in figure 16. As was the case at the cruise condition, the WBPPW analyses only partially reflect the nacelle-pylon effects; the modified nacelle shows slightly better agreement with the wind-tunnel data. Next, the redesigned DISC wing with the modified nacelle was analyzed at Mach 0.7. Figure 17 shows the resulting wing pressures and calculations for the baseline wing-body configuration with and without the modified nacelle. The pressures for the redesigned wing match those for the clean wing-body configuration very closely. Thus, even though the new wing is a point design, the design goal of removing the effect of the nacelle on the wing pressures appears to hold, even at off-design conditions.

Concluding Remarks

The current study explores the use of a direct/iterative design method for the reduction of drag for transport configurations, including those with engine nacelles. The method requires a target-pressure distribution as input and then develops a corresponding airfoil section. The method can be applied to two-dimensional airfoil sections or to three-dimensional wings. The three test cases that are shown demonstrate the use of the method for reducing drag; two types of nacelle integration problems are included.

The first case demonstrates the use of this method to design to an elliptic span-load distribution and to reduce wave drag by decreasing the shock strength while maintaining the elliptical span-load distribution. For this case, designing to an elliptic span-load distribution slightly decreased the induced drag, but it also slightly increased the wave drag. Decreasing wave drag produced a greater drag savings than decreasing induced drag and resulted in an overall reduction in drag coefficient of 0.0033.

In the second case, an overwing nacelle is added to the final configuration from the previous case; this nacelle has a significant effect on the performance of the configuration. The design method is successfully used to remove the inviscid drag that is produced by adding the nacelle and to return to an elliptic span-load distribution with reduced shock strength. For this case, the sum of the wave drag coefficient and induced drag coefficient is decreased by 0.0141.

In the third case, nacelle interference is eliminated by designing a wing-nacelle combination to reach clean-wing, target-pressure distributions. For this configuration, adding the nacelle to the clean wing makes only a slight difference in computed inviscid drag, so recontouring does not produce notable drag reductions. The design method is successful in returning the lower surface pressures to the clean-wing distribution and thus eliminates the interference of the nacelle.

These cases illustrate several possible uses of the method for reducing different types of drag. These designs are typically point designs valid for only one specific set of flow conditions. Additional analyses, as demonstrated in the third case, may verify that the designs are improvements over a range of conditions. The magnitude of the drag reduction obtained varies with the constraints of the problem and the configuration to be modified when the code is applied.

NASA Langley Research Center
Hampton, VA 23681-0001
August 7, 1992

References

Anon. 1980: Round Table Discussion. *Subsonic/Transonic Configuration Aerodynamics,* AGARD-CP-285, pp. RTD-4–RTD-17.

Anon. 1990: Specialists' Meeting on Computational Methods for Aerodynamic Design (Inverse) & Optimization. *Computational Methods for Aerodynamic Design (Inverse) and Optimization,* AGARD-CP-463, pp. RTD-1–RTD-6.

Boppe, Charles W. 1987: *Aerodynamic Analysis for Aircraft With Nacelles, Pylons, and Winglets at Transonic Speeds.* NASA CR-4066.

Bradshaw, P.; and Ferriss, D. H. 1971: Calculation of Boundary-Layer Development Using the Turbulent Energy Equation: Compressible Flow on Adiabatic Walls. *J. Fluid Mech.,* vol. 46, pt. 1, pp. 83–110.

Campbell, Richard L.; and Smith, Leigh A. 1987: A Hybrid Algorithm for Transonic Airfoil and Wing Design. *A Collection of Technical Papers—AIAA 5th Applied Aerodynamics Conference,* American Inst. of Aeronautics and Astronautics, pp. 527–538. (Available as AIAA-87-2552.)

Giles, Michael; and Drela, Mark 1986: A Two-Dimensional Transonic Aerodynamic Design Method. *A Collection of Technical Papers—AIAA 4th Applied Aerodynamics Conference,* American Inst. of Aeronautics and Astronautics, pp. 197–204. (Available as AIAA-86-1793.)

Haines, A. B. 1987: 27th Lanchester Memorial Lecture—Scale Effect in Transonic Flow. *Aeronaut. J.,* vol. 91, no. 907, pp. 291–313.

Hicks, Raymond M.; Murman, Earll M.; and Vanderplaats, Garret N. 1974: *An Assessment of Airfoil Design by Numerical Optimization.* NASA TM X-3092.

Kennelly, Robert A., Jr. 1983: Improved Method for Transonic Airfoil Design-by-Optimization. AIAA-83-1864.

Lee, Edwin E., Jr.; and Pendergraft, Odis C., Jr. 1985: *Installation Effects of Long-Duct Pylon-Mounted Nacelles on a Twin-Jet Transport Model With Swept Supercritical Wing.* NASA TP-2457.

Lock, R. C. 1985: Prediction of the Drag of Wings at Subsonic Speeds by Viscous/Inviscid Interaction Techniques. *Aircraft Drag Prediction and Reduction,* AGARD-R-723, pp. 10-1 10-71.

Smith, Leigh Ann; and Campbell, Richard L. 1991: *A Method for the Design of Transonic Flexible Wings.* NASA TP-3045.

Sobieczky, H.; Yu, N. J.; Fung, K.-Y.; and Seebass, A. R. 1979: New Method for Designing Shock-Free Transonic Configurations. *AIAA J.,* vol. 17, no. 7, pp. 722–729.

Volpe, G.; and Melnik, R. E. 1985: A Method for Designing Closed Airfoils for Arbitrary Supercritical Speed Distributions. AIAA-85-5023.

Volpe, G. 1990: Inverse Design of Airfoil Contours: Constraints, Numerical Method, and Applications. *Computational Methods for Aerodynamic Design (Inverse) and Optimization,* AGARD-CP-463, pp. 4-1–4-18.

Waggoner, E. G. 1980: Computational Transonic Analysis for a Supercritical Transport Wing-Body Configuration. AIAA-80-0129.

Table 1. Clean-Wing Drag Coefficients

Drag	Baseline configuration	TTE approach	DISC approach
Induced	0.0140	0.0136	0.0136
Wave	.0045	.0047	.0016
Total	0.0185	0.0183	0.0152

Table 2. Wing-Nacelle Drag Coefficients

Drag	Baseline configuration	DISC approach
Induced	0.0150	0.0132
Wave	.0124	.0001
Total	0.0274	0.0133

Table 3. High-Wing Transport Drag Coefficients

Drag	Baseline configuration	DISC approach
Induced	0.0192	0.0192
Wave	.0015	.0012
Total	0.0207	0.0204

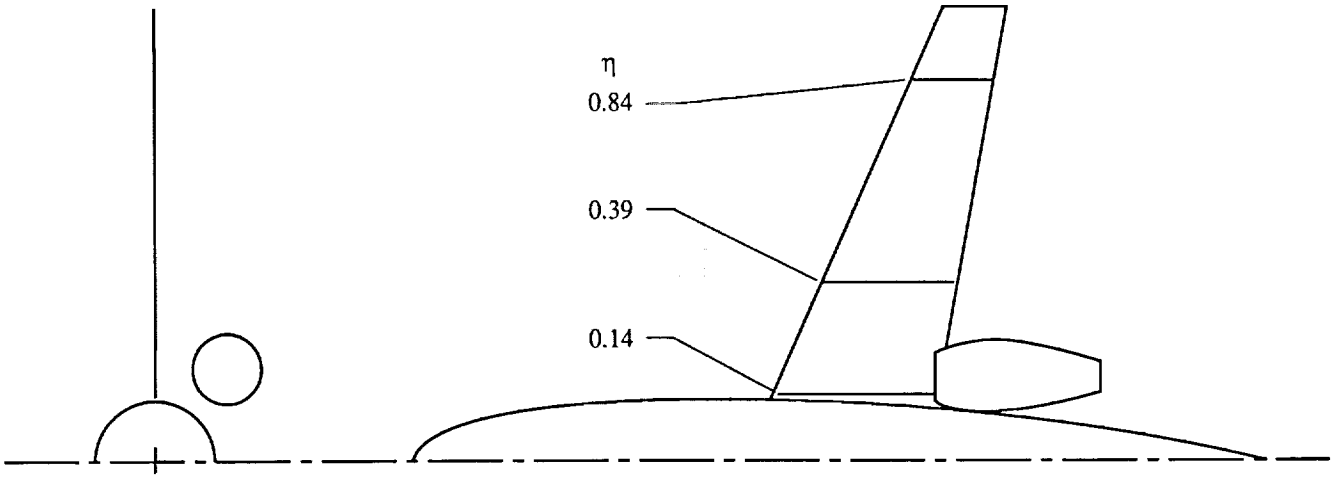

Figure 1. Executive-jet planform.

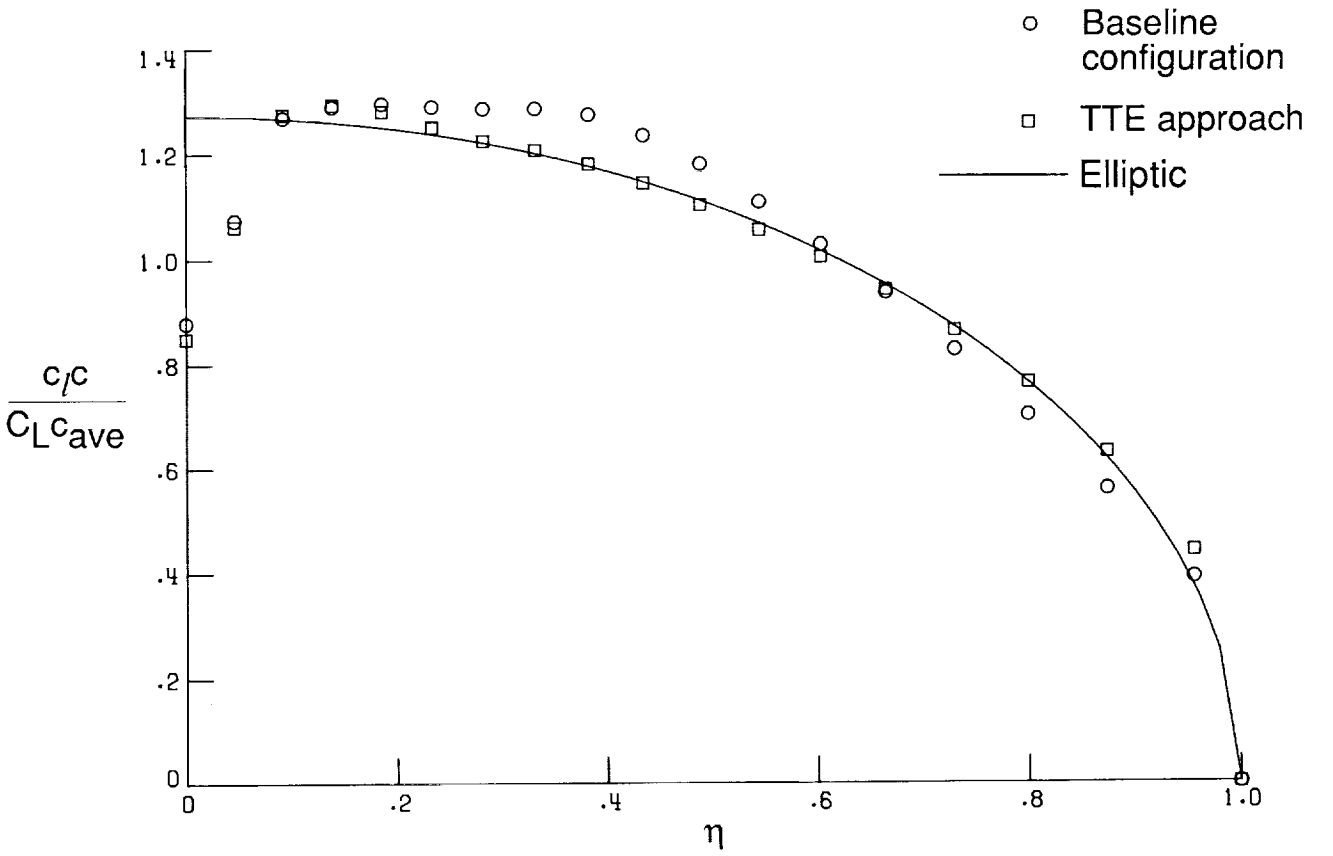

Figure 2. Use of twisting to obtain elliptic span load. $M = 0.79$.

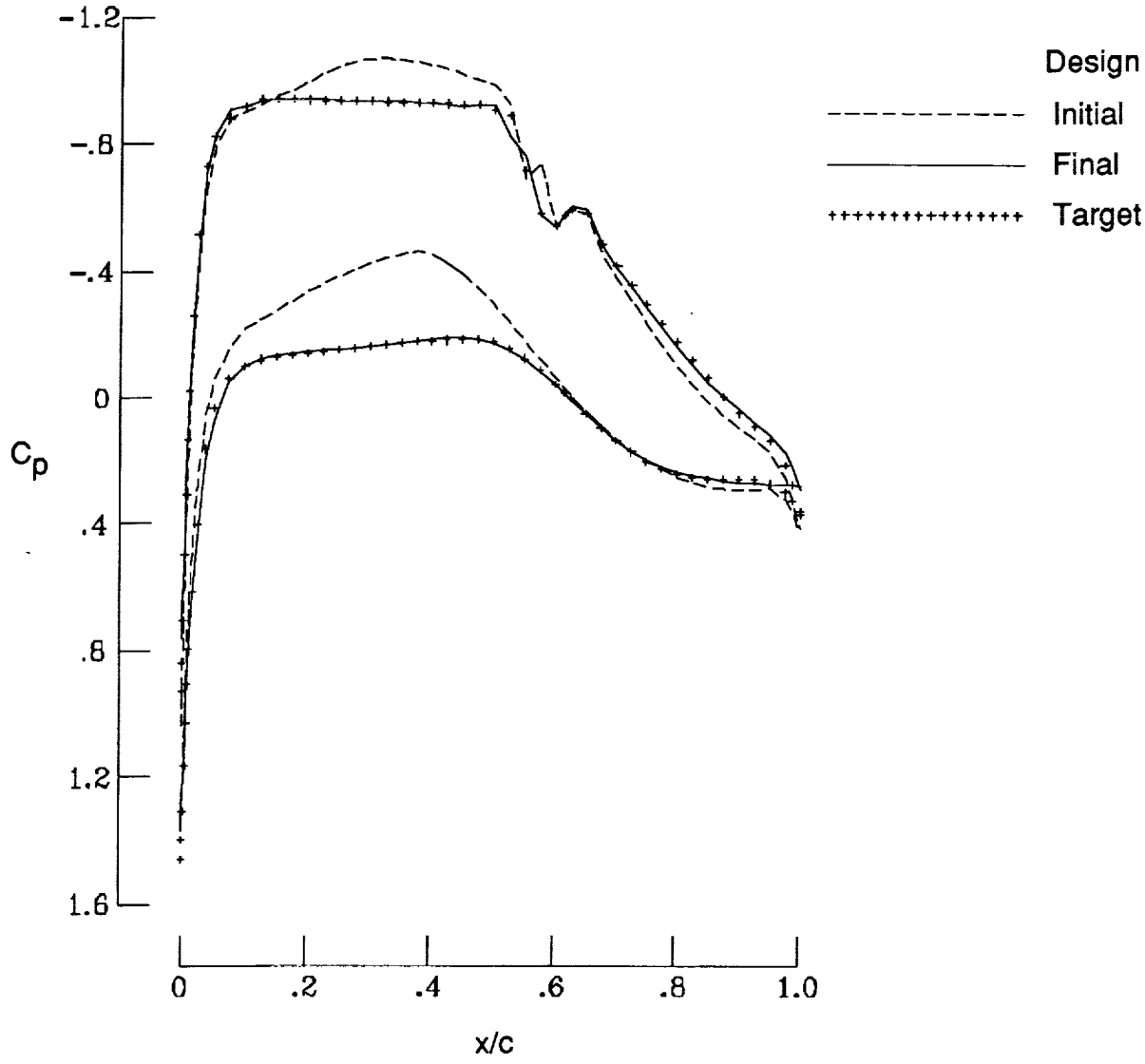

Figure 3. Typical design results.

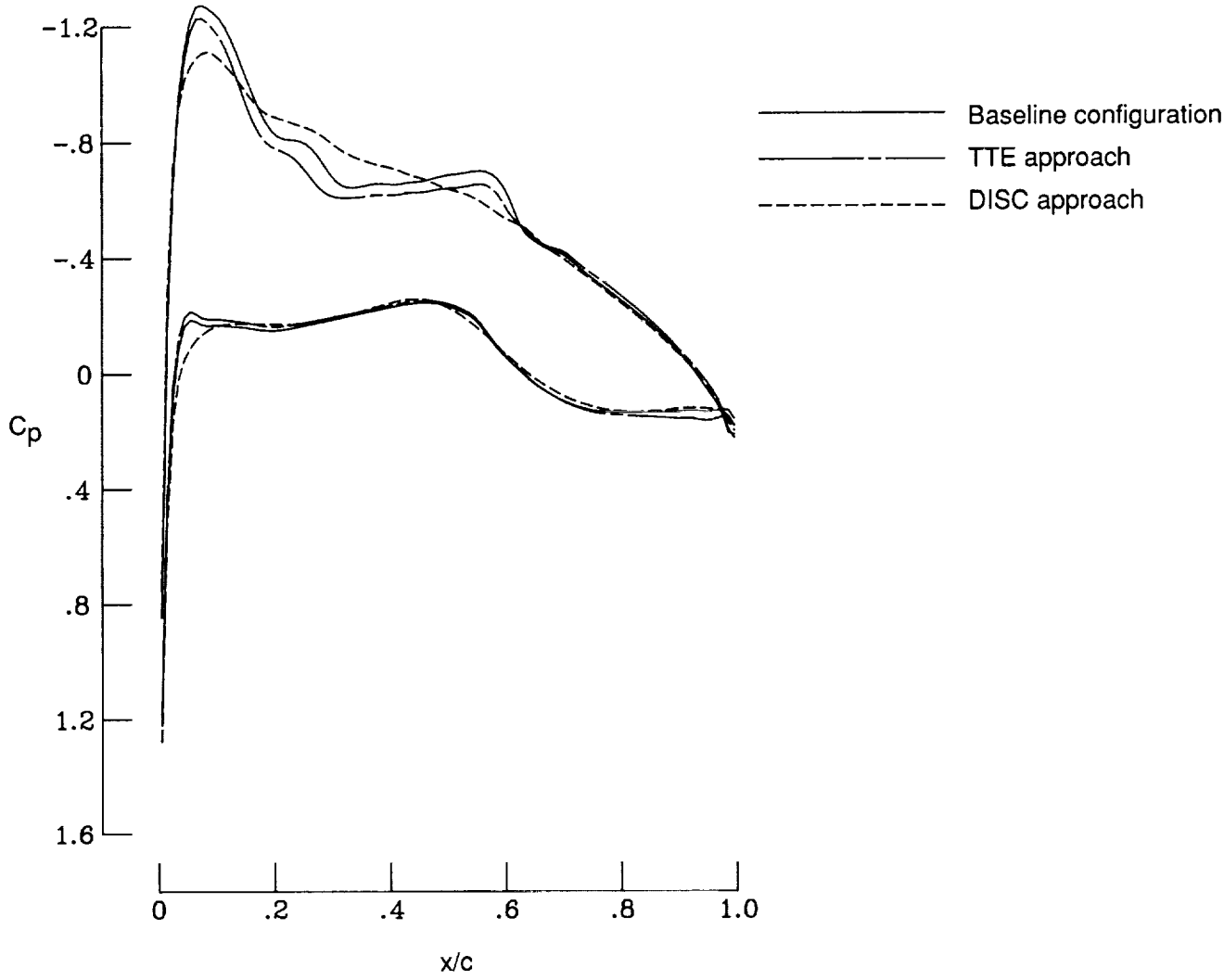

(a) $\eta = 0.14$.

Figure 4. Executive-jet wing redesign and pressure coefficient comparisons. $M = 0.79$.

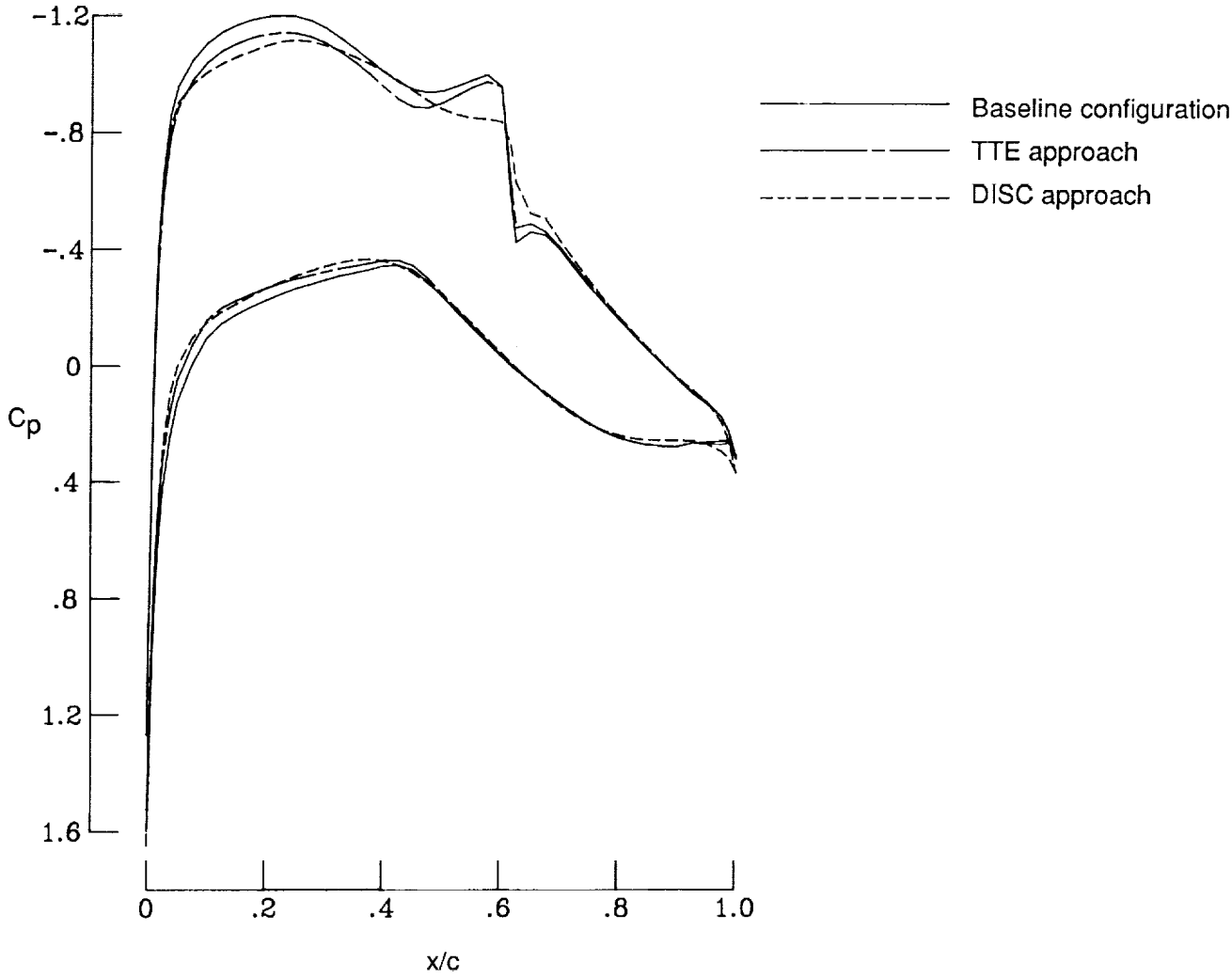

(b) $\eta = 0.39$.

Figure 4. Continued.

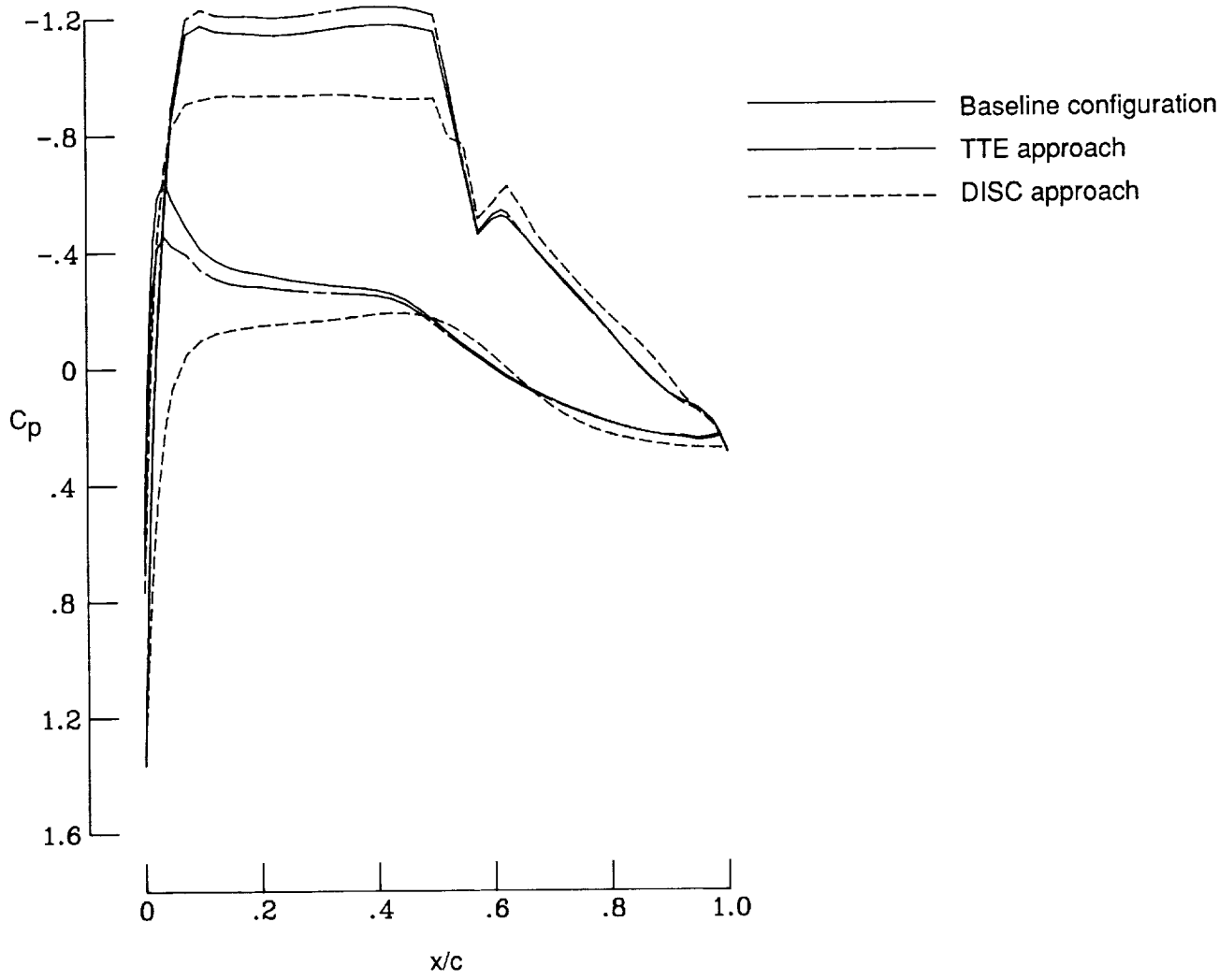

(c) $\eta = 0.84$.

Figure 4. Concluded.

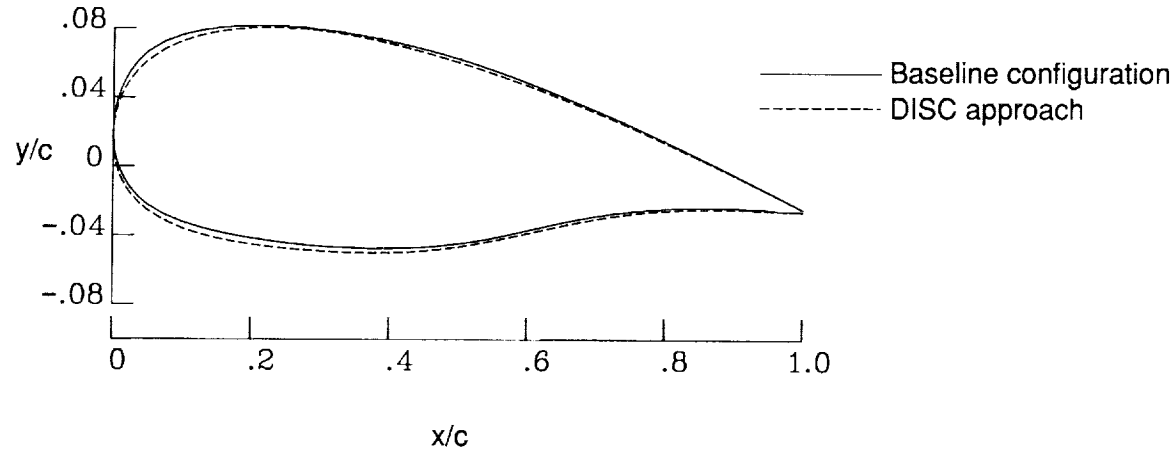

(a) $\eta = 0.14$.

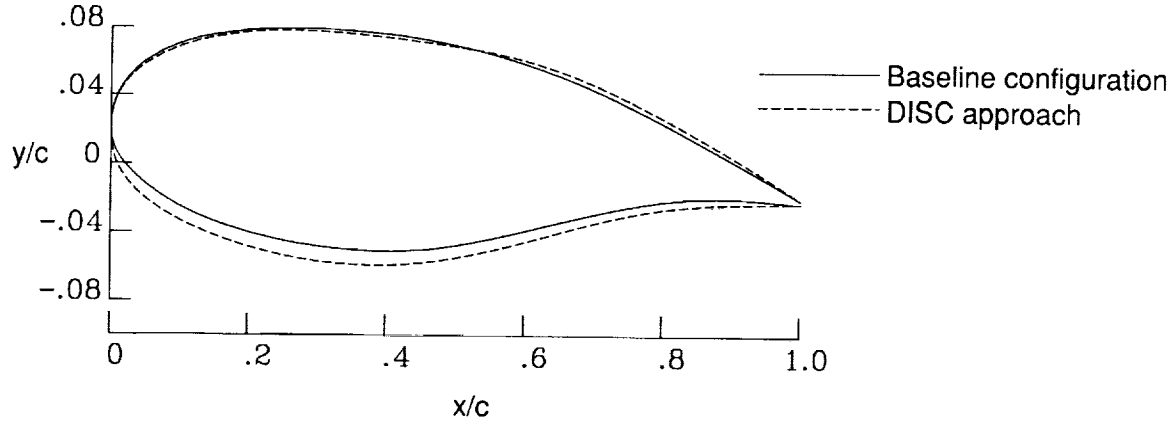

(b) $\eta = 0.39$.

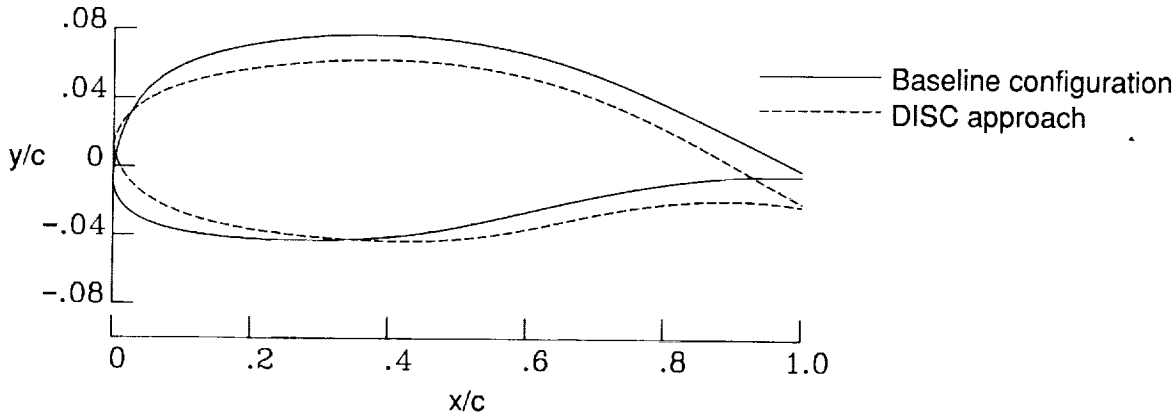

(c) $\eta = 0.84$.

Figure 5. Executive-jet wing redesign and geometry comparisons. $M = 0.79$.

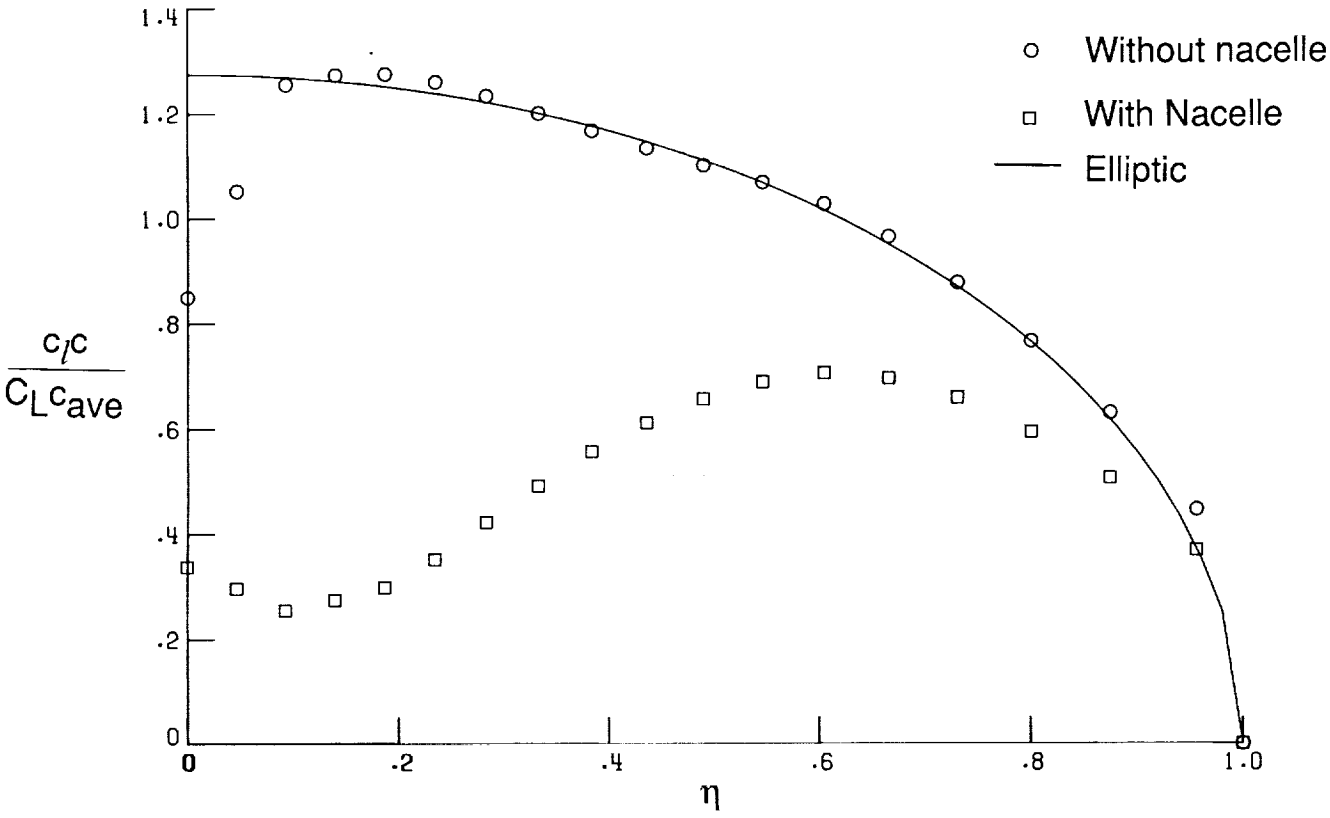

Figure 6. Effect of nacelle on DISC (case 1) wing.

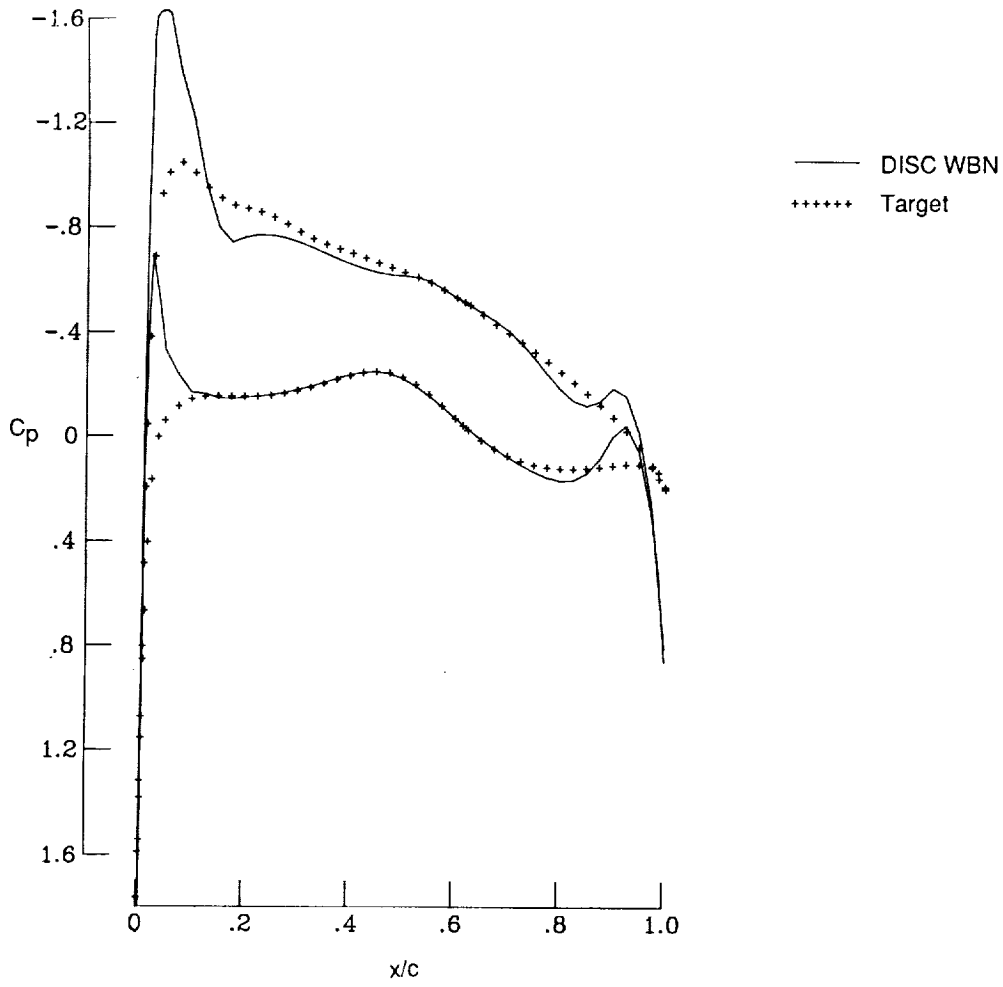

(a) Pressure coefficients.

Figure 7. Nacelle-on design to reach clean-wing targets. $\eta = 0.12$.

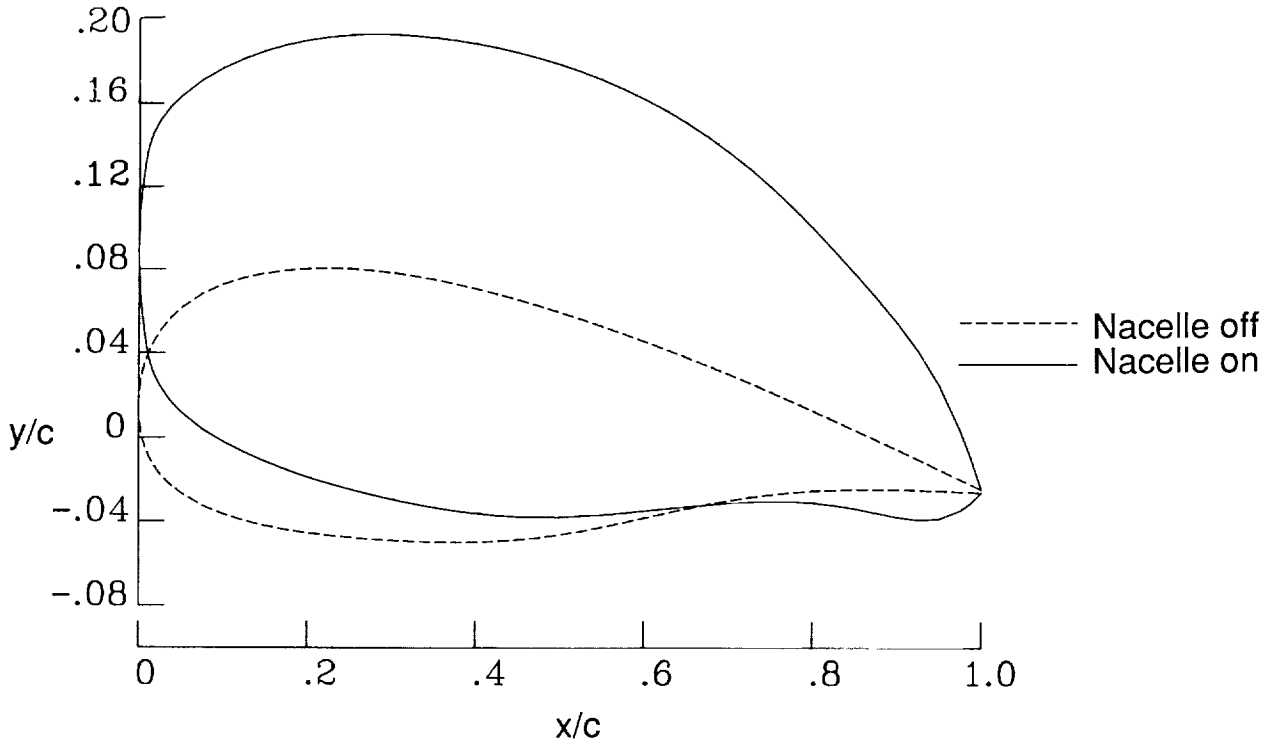

(b) Airfoil geometry.

Figure 7. Concluded.

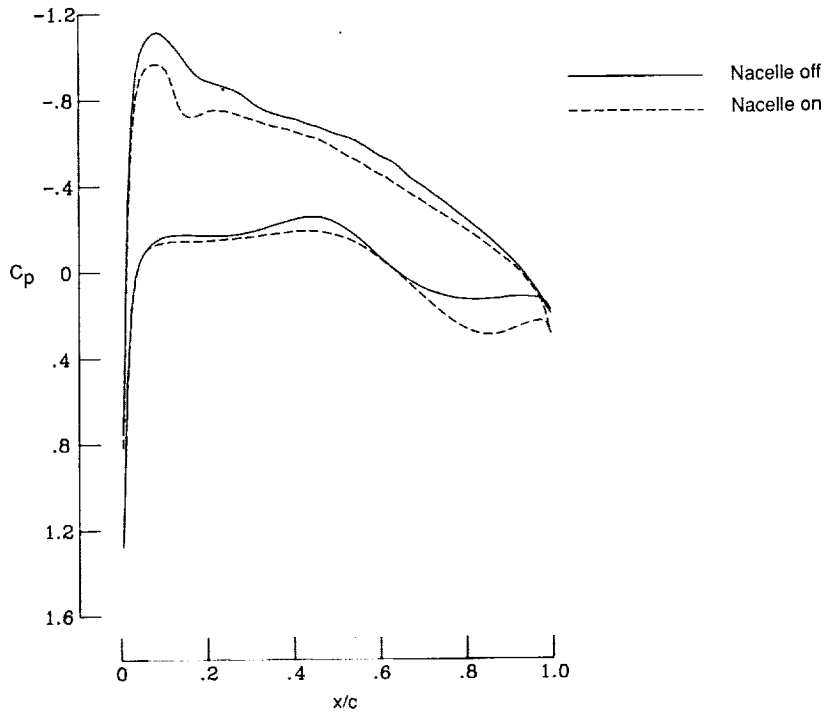

(a) $\eta = 0.14$.

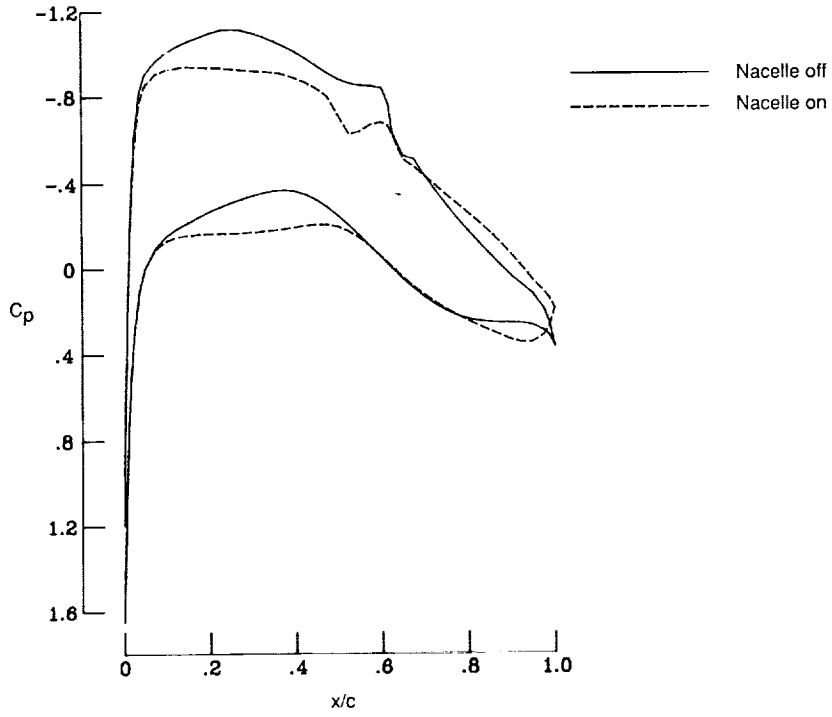

(b) $\eta = 0.39$.

Figure 8. Executive-jet wing analysis of nacelle-on and nacelle-off designs with pressure coefficient comparisons. $M = 0.79$.

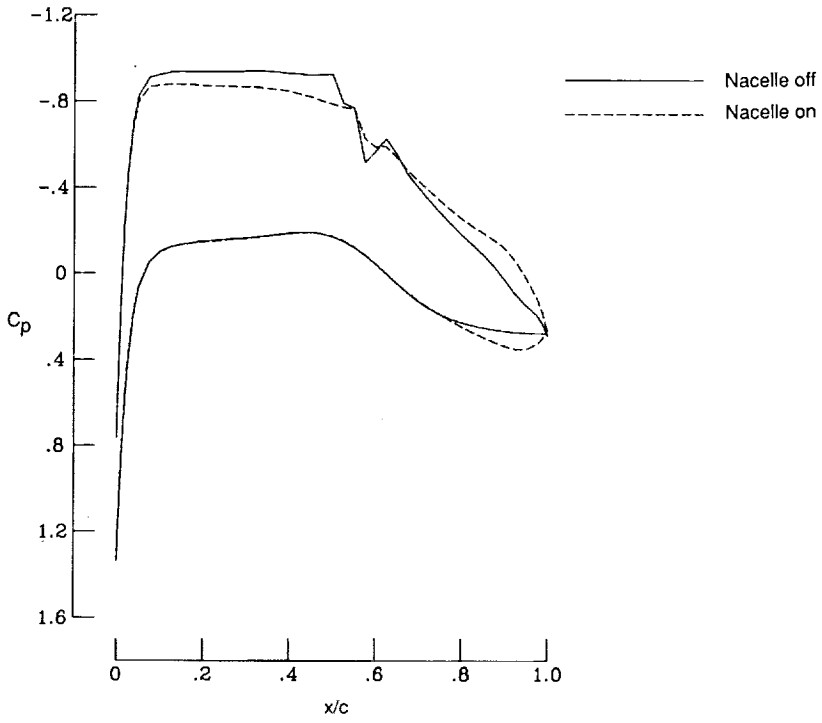

(c) $\eta = 0.84$.

Figure 8. Concluded.

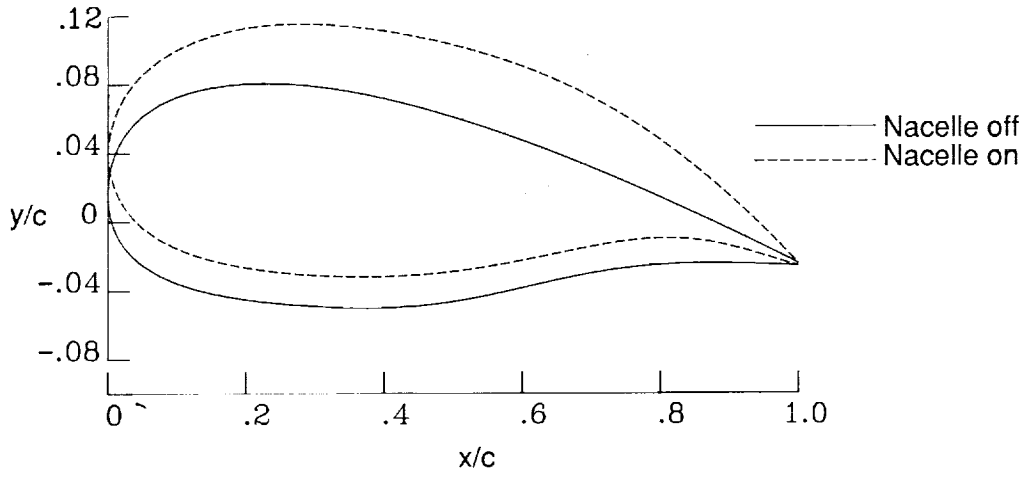

(a) $\eta = 0.14$.

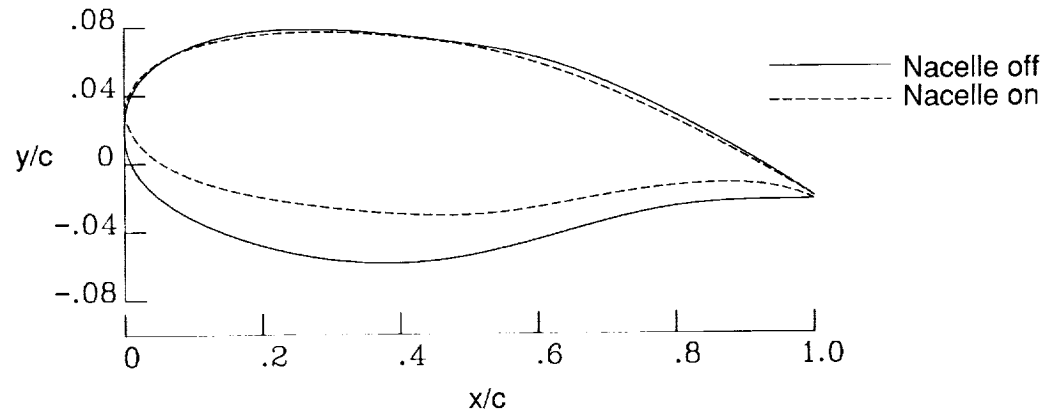

(b) $\eta = 0.39$.

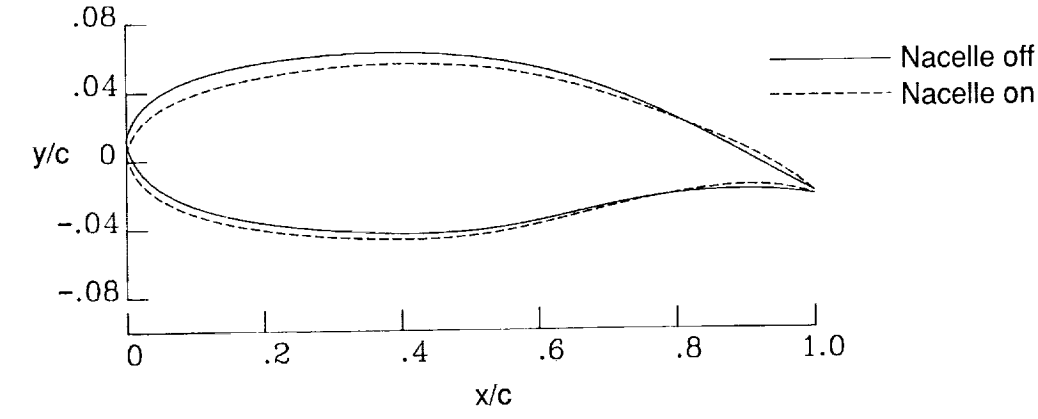

(c) $\eta = 0.84$.

Figure 9. Executive-jet wing analysis of nacelle-on and nacelle-off designs with geometry comparisons. $M = 0.79$.

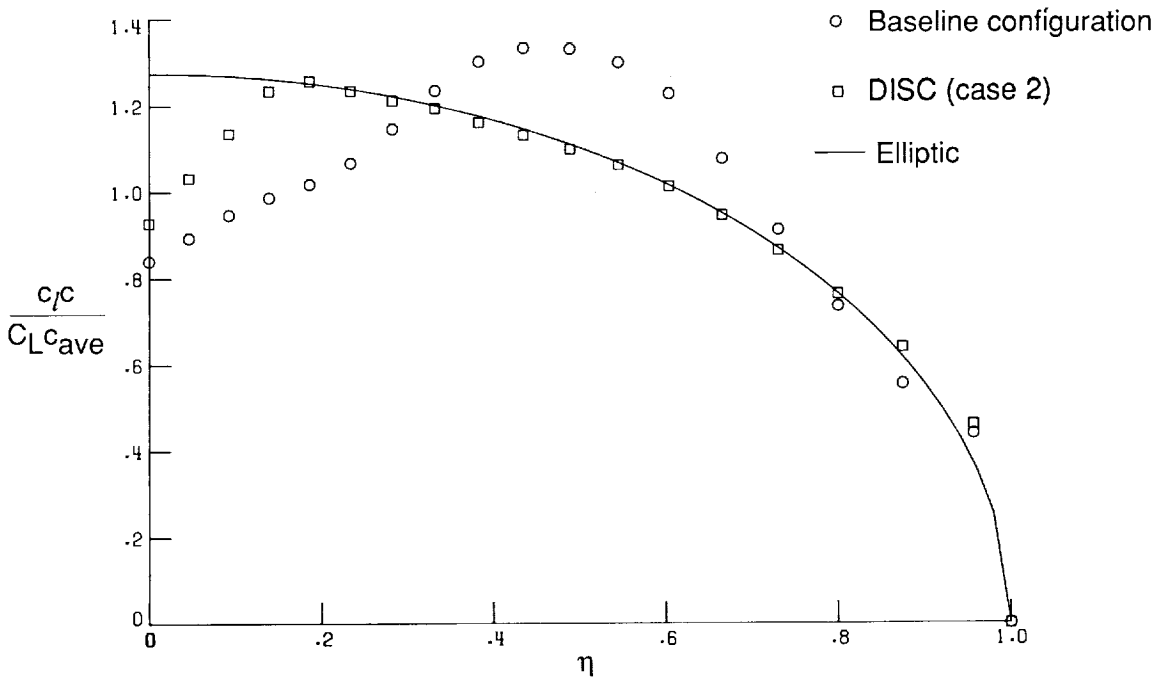

Figure 10. Span load for redesigned executive-jet wing with nacelle. $M = 0.79; C_L = 0.55$.

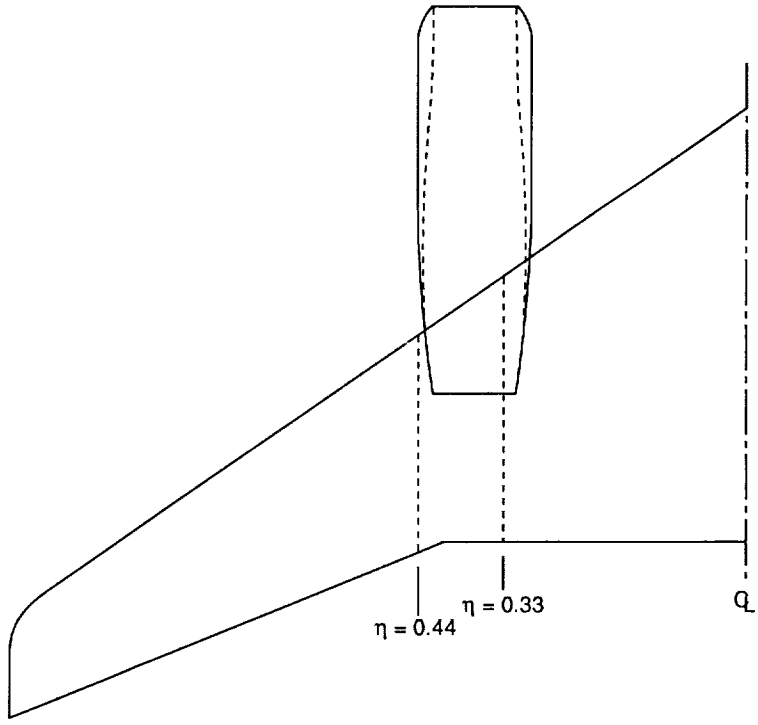

Figure 11. Planform of high-wing transport.

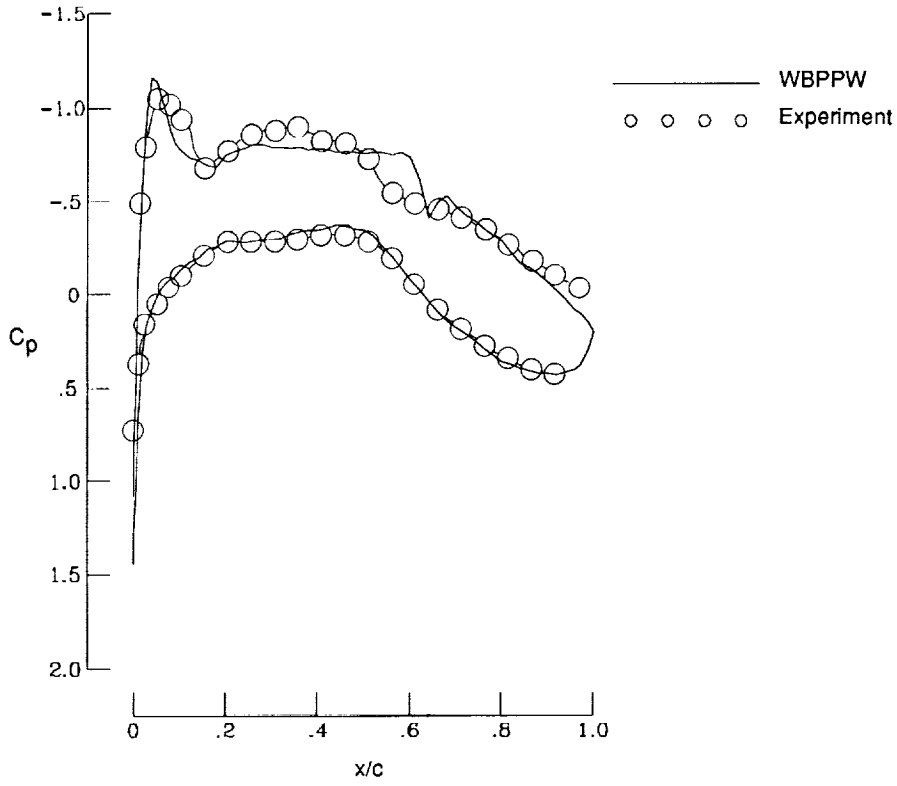

(a) $\eta = 0.25$.

Figure 12. Comparison of theoretical pressure coefficients with experimental data for nacelle-off high-wing transport. $M = 0.807$.

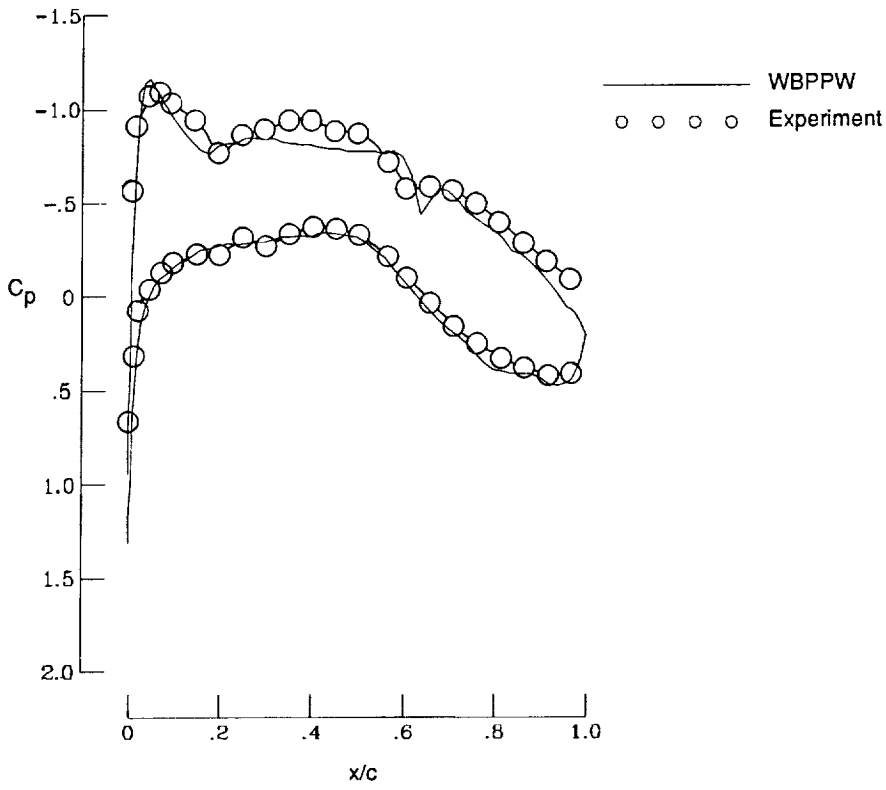

(b) $\eta = 0.33$.

Figure 12. Continued.

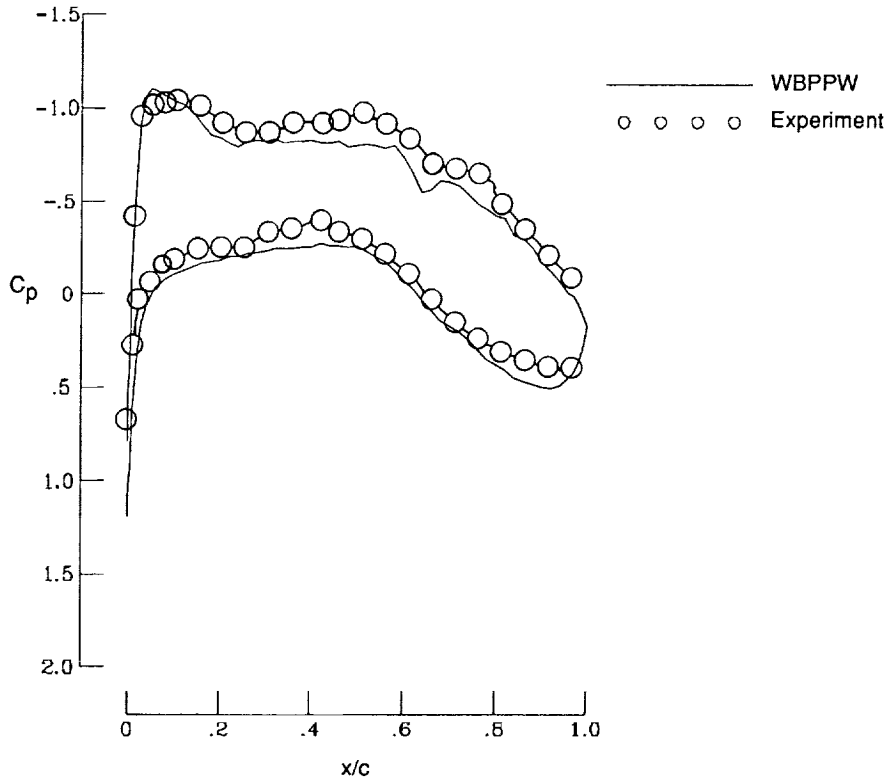

(c) $\eta = 0.44$.

Figure 12. Concluded.

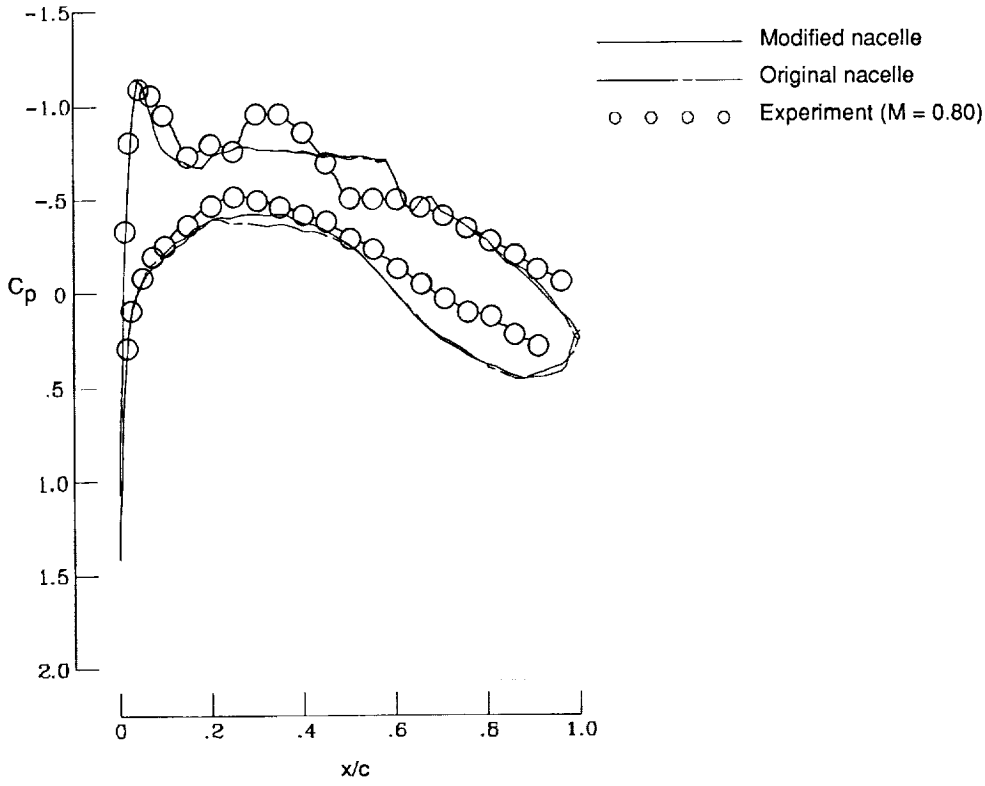

(a) $\eta = 0.25$.

Figure 13. Comparison of original and modified nacelle theoretical pressure coefficients with experimental data for high-wing transport. $M = 0.807$.

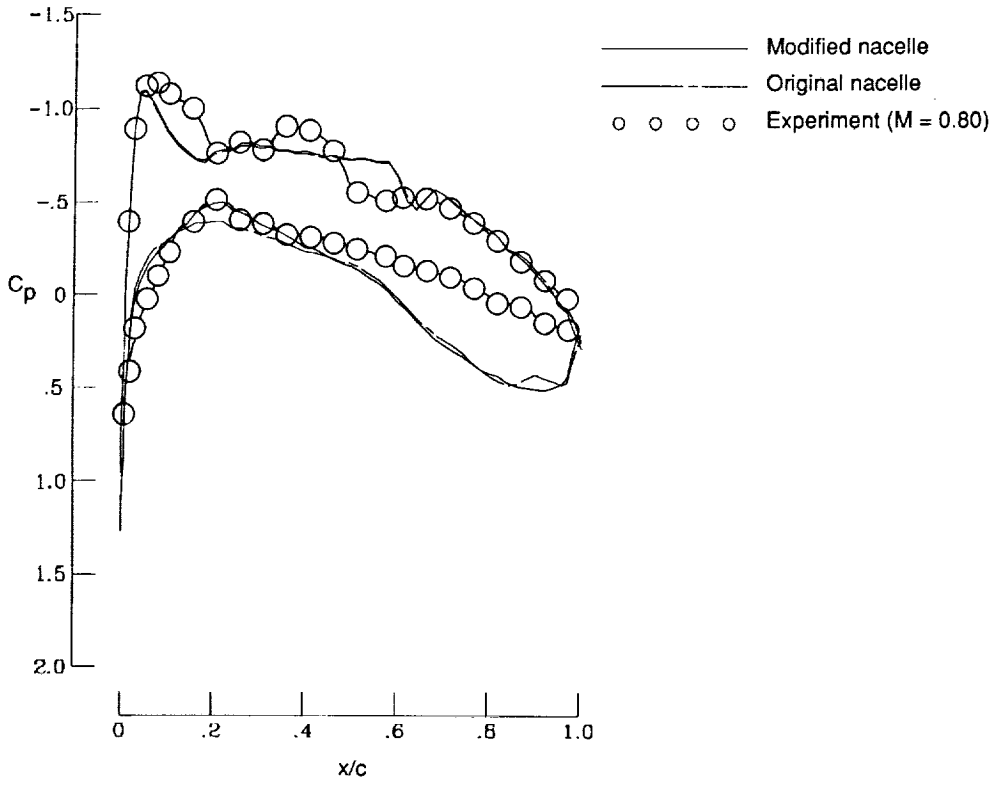

(b) $\eta = 0.33$.

Figure 13. Continued.

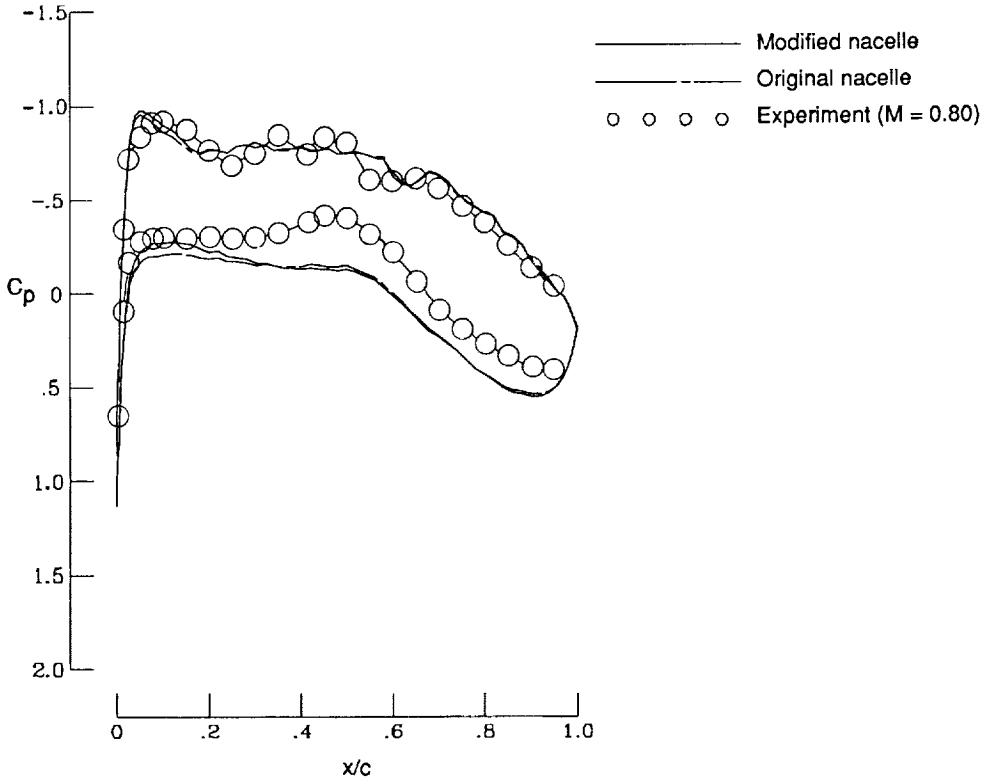

(c) $\eta = 0.44$.

Figure 13. Concluded.

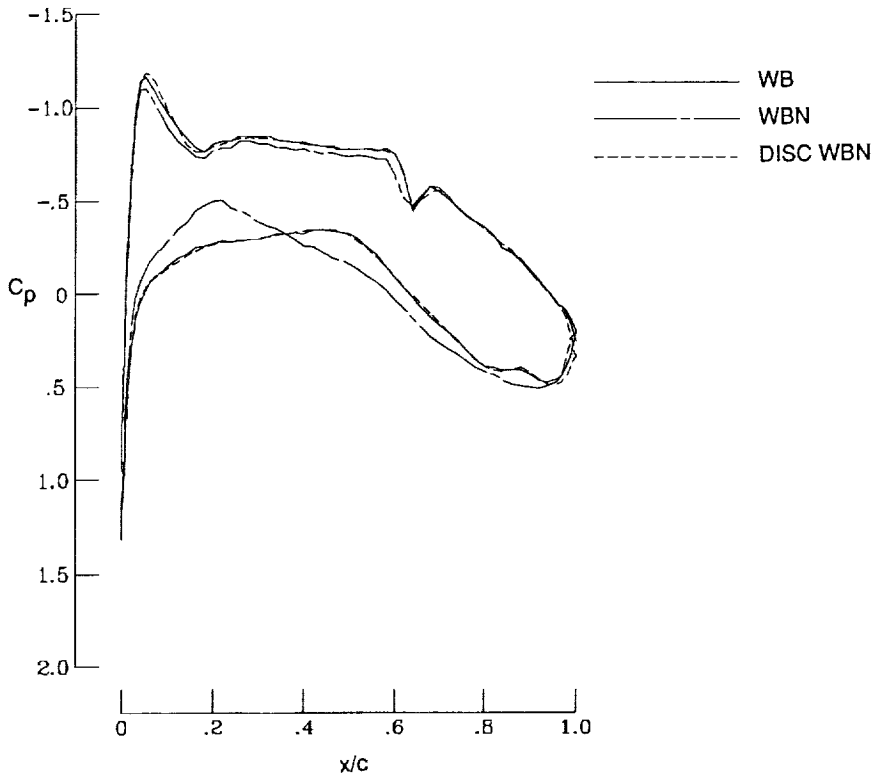

(a) $\eta = 0.33$; inboard of nacelle.

Figure 14. Pressure coefficient comparisons for redesign of high-wing transport. $M = 0.807$.

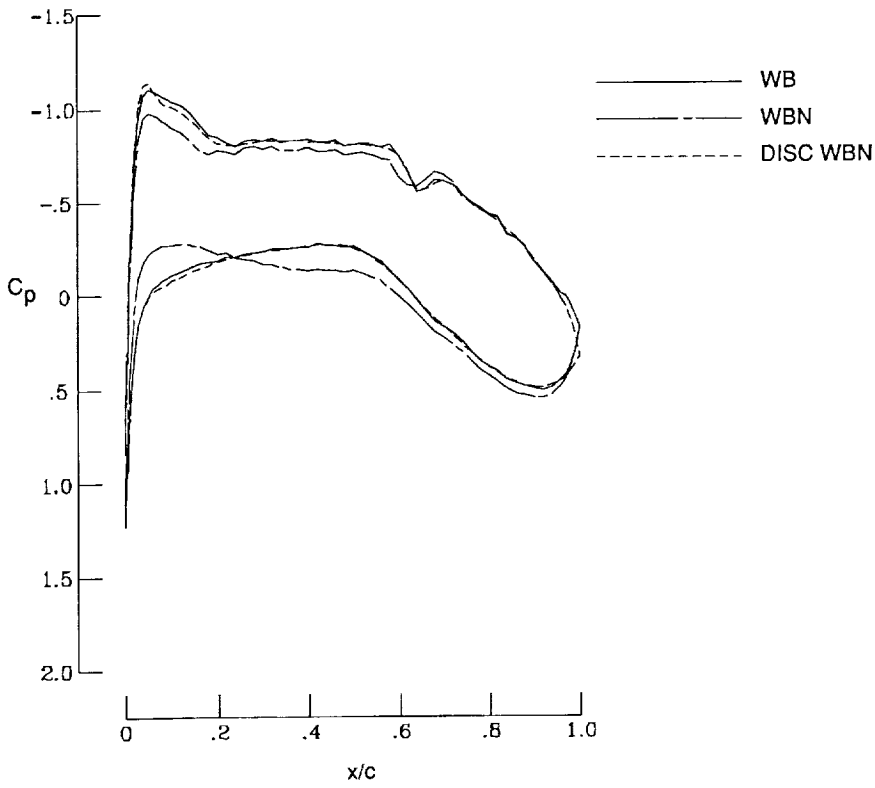

(b) $\eta = 0.44$; outboard of nacelle.

Figure 14. Concluded.

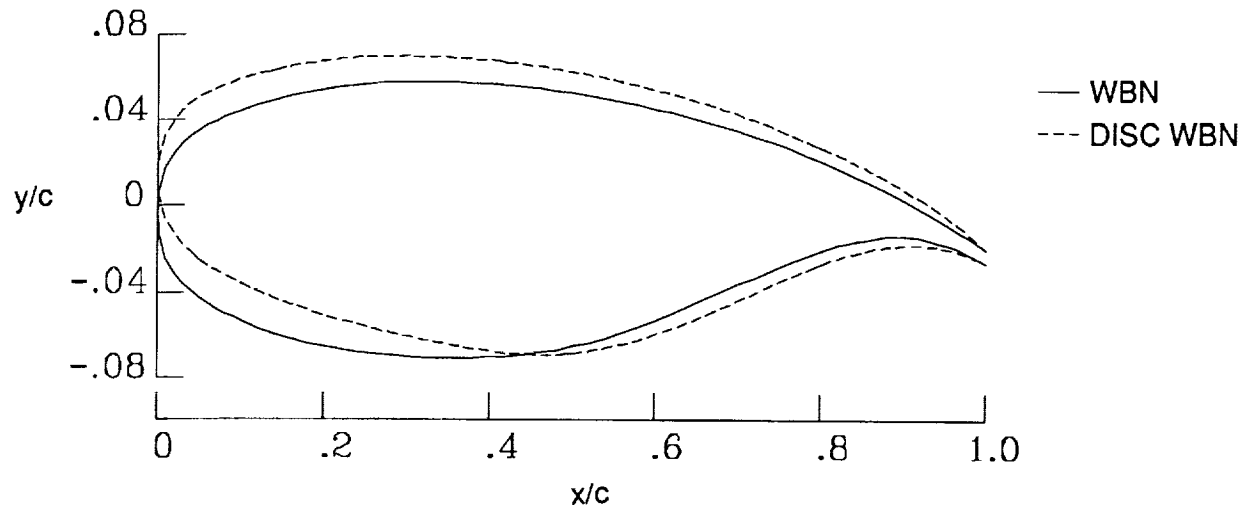

(a) $\eta = 0.33$; inboard of nacelle.

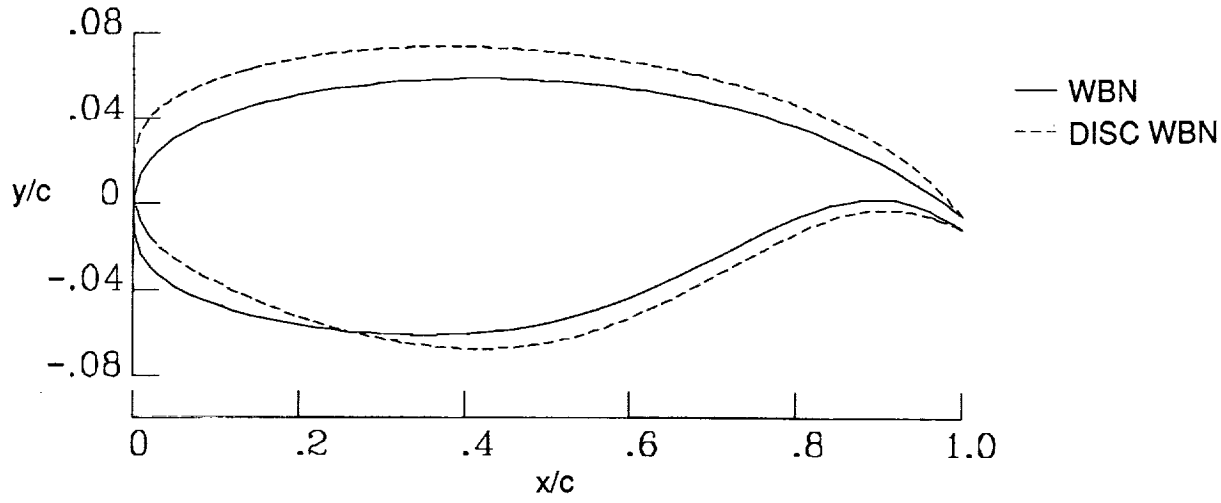

(b) $\eta = 0.44$; outboard of nacelle.

Figure 15. Airfoil geometry comparisons for redesign of high-wing transport.

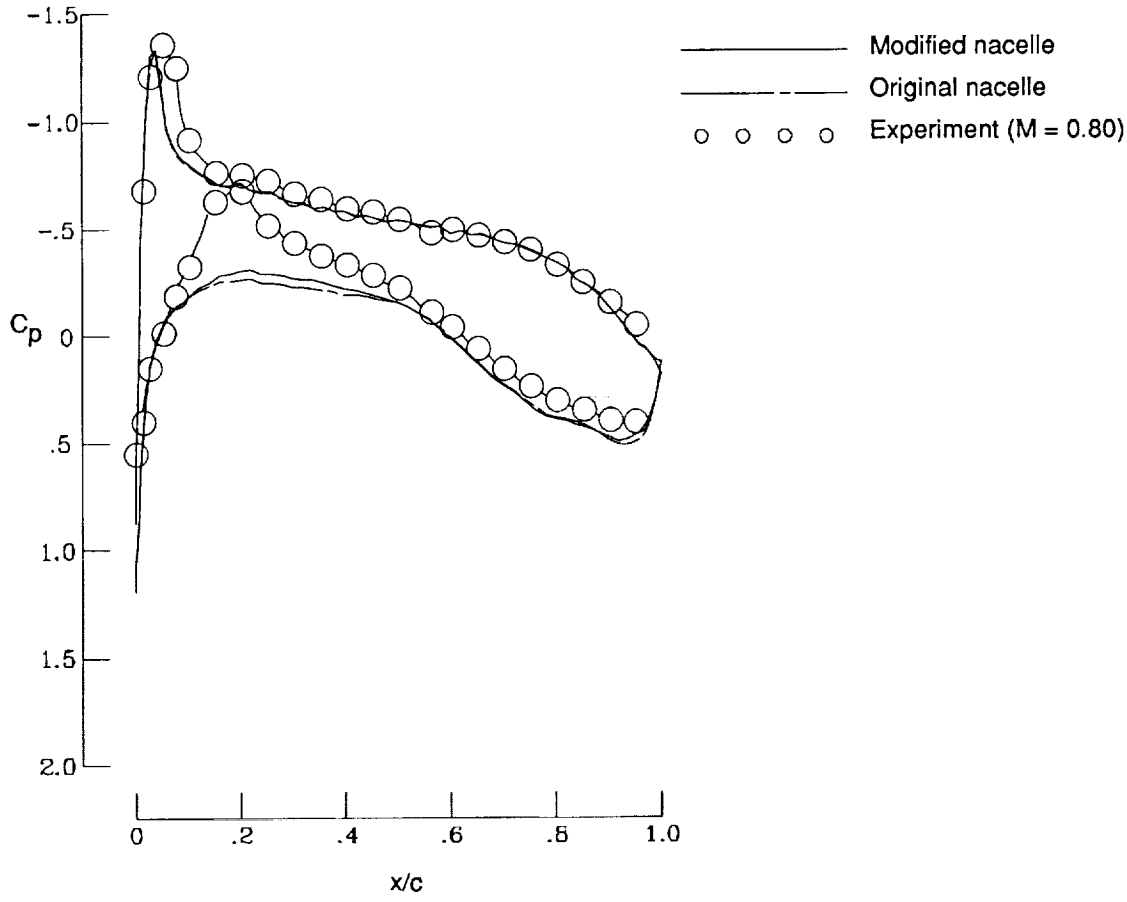

Figure 16. Comparison of computational and experimental analyses at off-design conditions for high-wing transport. $M = 0.70$; $\eta = 0.33$.

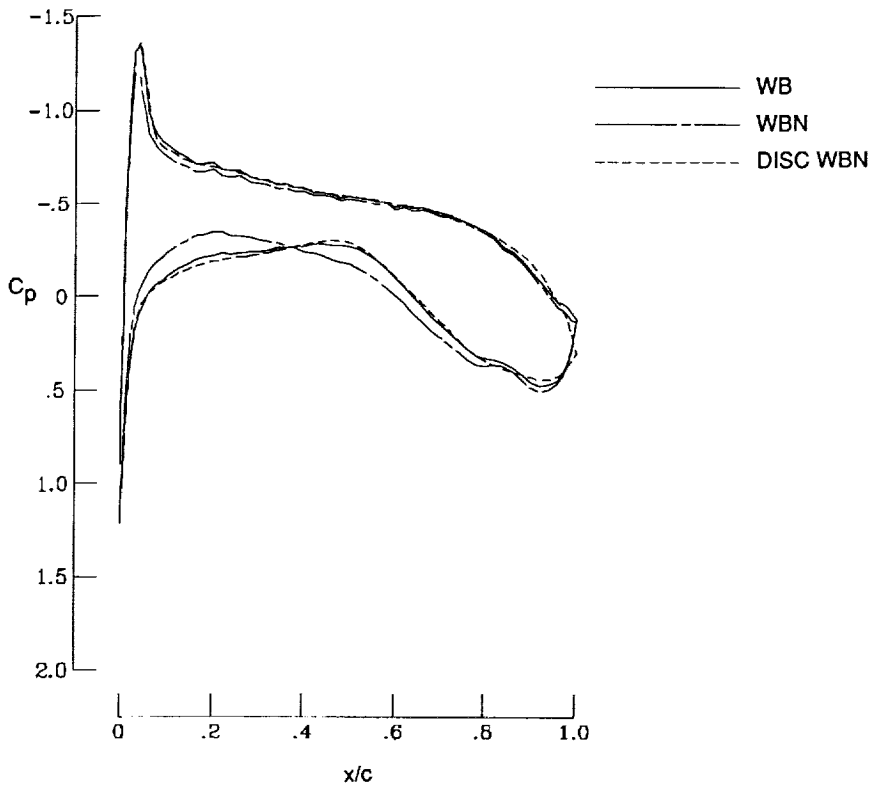

(a) $\eta = 0.33$; inboard of nacelle.

Figure 17. Off-design analysis of high-wing transport. $M = 0.70$.

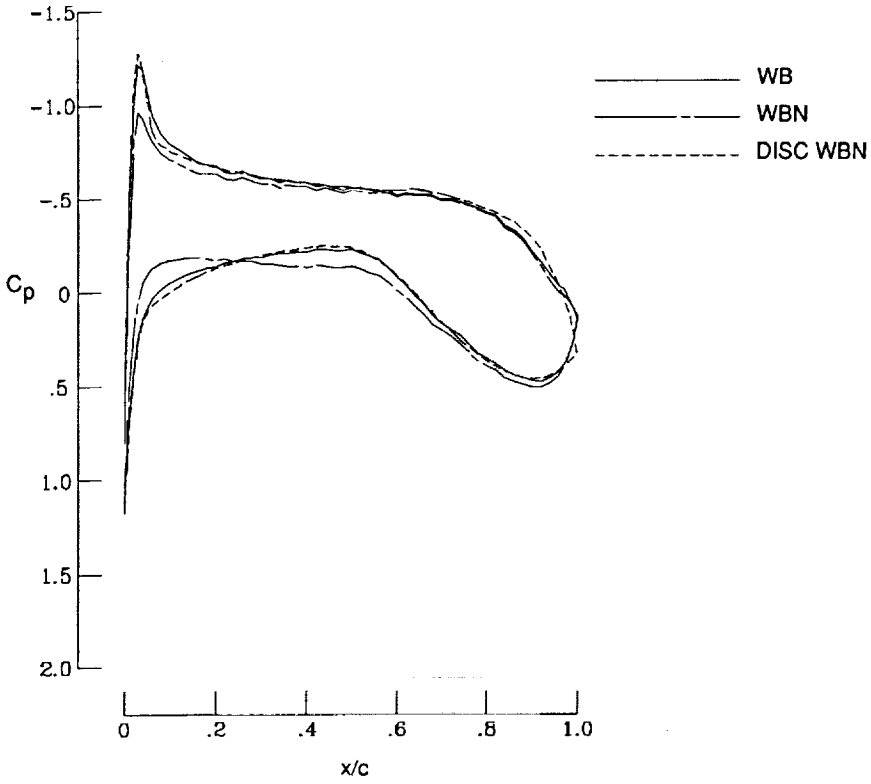

(b) $\eta = 0.44$; outboard of nacelle.

Figure 17. Concluded.

REPORT DOCUMENTATION PAGE

Form Approved
OMB No. 0704-0188

1. AGENCY USE ONLY *(Leave blank)*	2. REPORT DATE	3. REPORT TYPE AND DATES COVERED
	September 1992	Technical Paper

4. TITLE AND SUBTITLE
Applications of a Direct/Iterative Design Method to Complex Transonic Configurations

5. FUNDING NUMBERS
WU 505-59-10-03

6. AUTHOR(S)
Leigh Ann Smith and Richard L. Campbell

7. PERFORMING ORGANIZATION NAME(S) AND ADDRESS(ES)
NASA Langley Research Center
Hampton, VA 23681-0001

8. PERFORMING ORGANIZATION REPORT NUMBER
L-16962

9. SPONSORING/MONITORING AGENCY NAME(S) AND ADDRESS(ES)
National Aeronautics and Space Administration
Washington, DC 20546-0001

10. SPONSORING/MONITORING AGENCY REPORT NUMBER
NASA TP-3234

11. SUPPLEMENTARY NOTES

12a. DISTRIBUTION/AVAILABILITY STATEMENT
Unclassified Unlimited

Subject Category 02

12b. DISTRIBUTION CODE

13. ABSTRACT *(Maximum 200 words)*

The current study explores the use of an automated direct/iterative design method for the reduction of drag for transport configurations, including configurations with engine nacelles. The method requires the user to choose a proper target-pressure distribution and then develops a corresponding airfoil section. The method can be applied to two-dimensional airfoil sections or to three-dimensional wings. The three cases that are presented show successful application of the method for reducing drag from various sources. The first two cases demonstrate the use of the method to reduce induced drag by designing to an elliptic span-load distribution and to reduce wave drag by decreasing the shock strength for a given lift. In the second case, a body-mounted nacelle is added and the method is successfully used to eliminate increases in wing drag associated with the nacelle addition by designing to an arbitrary pressure distribution that has an elliptic span-load distribution with reduced shock strength. The third case does not show a large drag decrease, but does demonstrate the elimination of nacelle influence on the original pressure distribution as a result of the redesigning of a wing in combination with a given underwing nacelle to clean-wing, target-pressure distributions. These cases illustrate several possible uses of the method for reducing different types of drag. The magnitude of the obtainable drag reduction varies with the constraints of the problem and the configuration to be modified.

14. SUBJECT TERMS
Aircraft design; Drag reduction; Transport aircraft; Nacelle interference

15. NUMBER OF PAGES
34

16. PRICE CODE
A03

17. SECURITY CLASSIFICATION OF REPORT	18. SECURITY CLASSIFICATION OF THIS PAGE	19. SECURITY CLASSIFICATION OF ABSTRACT	20. LIMITATION OF ABSTRACT
Unclassified	Unclassified		

NSN 7540-01-280-5500

Standard Form 298(Rev. 2-89)
Prescribed by ANSI Std. Z39-18
298-102

NASA-Langley, 1992